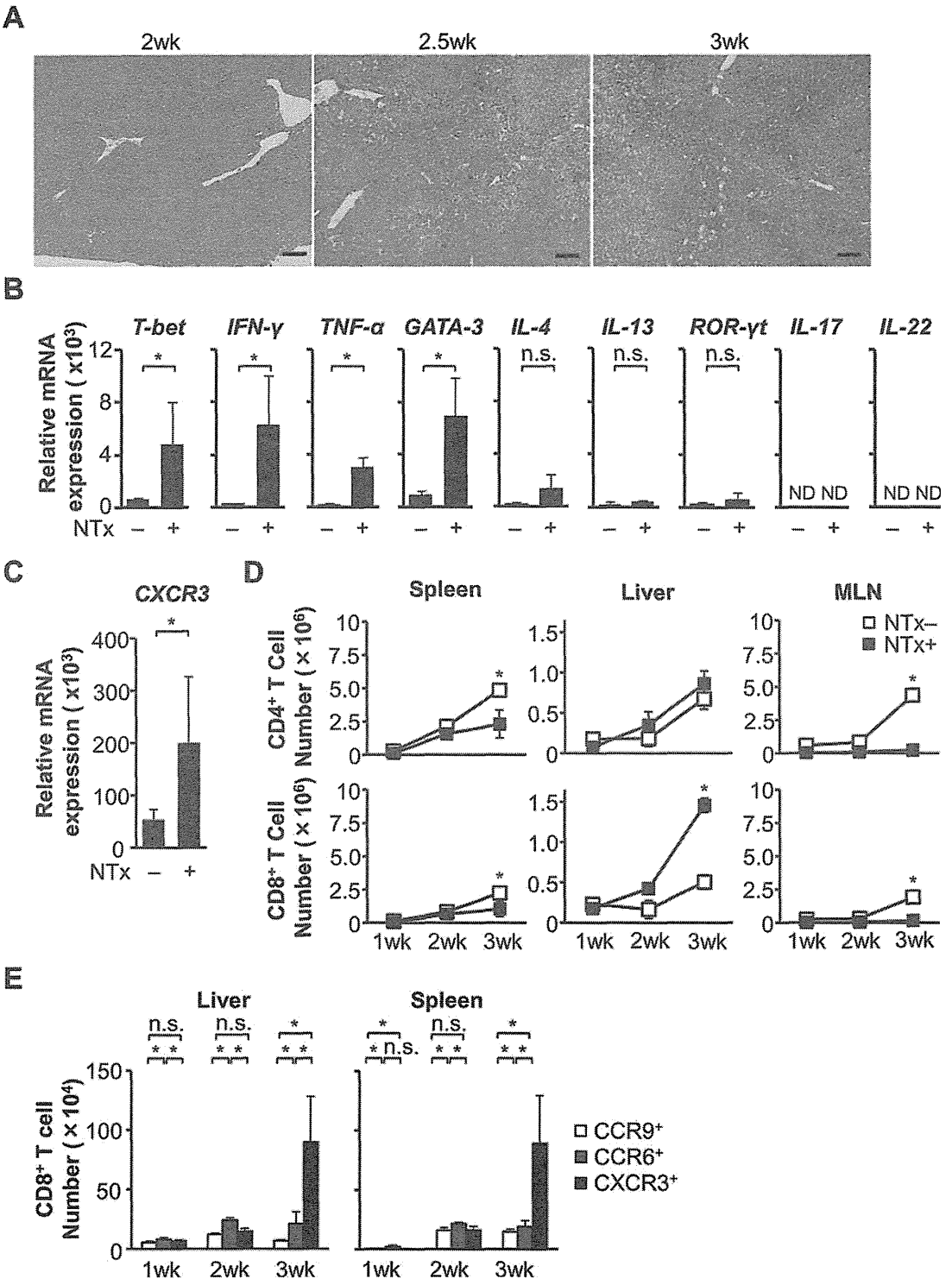

Fig. 1. Histological and immunological analysis of AIH-bearing NTx-*PD-1*$^{-/-}$ mice. (A) Histological findings of liver in NTx-*PD-1*$^{-/-}$ mice at indicated ages in weeks. All scale bars, 100 μm. (B and C) Livers from 3-week-old *PD-1*$^{-/-}$ mice with or without NTx were used for real-time qRT-PCR analyses for mRNA expressions of lineage-specific transcription factors, such as T-bet, GATA-3, or ROR-γt, and various cytokines (B) and Th1-cell–expressing chemokine receptor CXCR3 (C). (D) Cell numbers of CD4$^+$ and CD8$^+$ T cells in spleen, liver, and MLNs of *PD-1*$^{-/-}$ mice with or without NTx at the indicated age. Isolated cells were stained with FITC-anti-CD3e and APC-Cy7-anti-CD4 or APC-anti-CD8. (E) Cell numbers of splenic and hepatic CD8$^+$ T cells expressing indicate chemokine receptors. Isolated cells were stained with FITC-anti-CD3e, APC-anti-CD8 and PE-anti-CCR6, -anti-CCR9, or -anti-CXCR3. FCM analyses were carried out as described in the Supporting Materials and Methods. Numbers of indicated T cell populations were calculated by (percentage of the cells in viable cells) x (no. of viable cells). Data are shown as the mean of at least three mice. Error bars represent standard deviation. * indicate $P < 0.05$. n.s., not significant. ND, not detected. ROR-γt, retinoid-related orphan receptor-gamma t; FITC, fluorescein isothiocyanate; APC, allophyocyanin; Cy7, cyanine 7; PE, phycoerythrin.

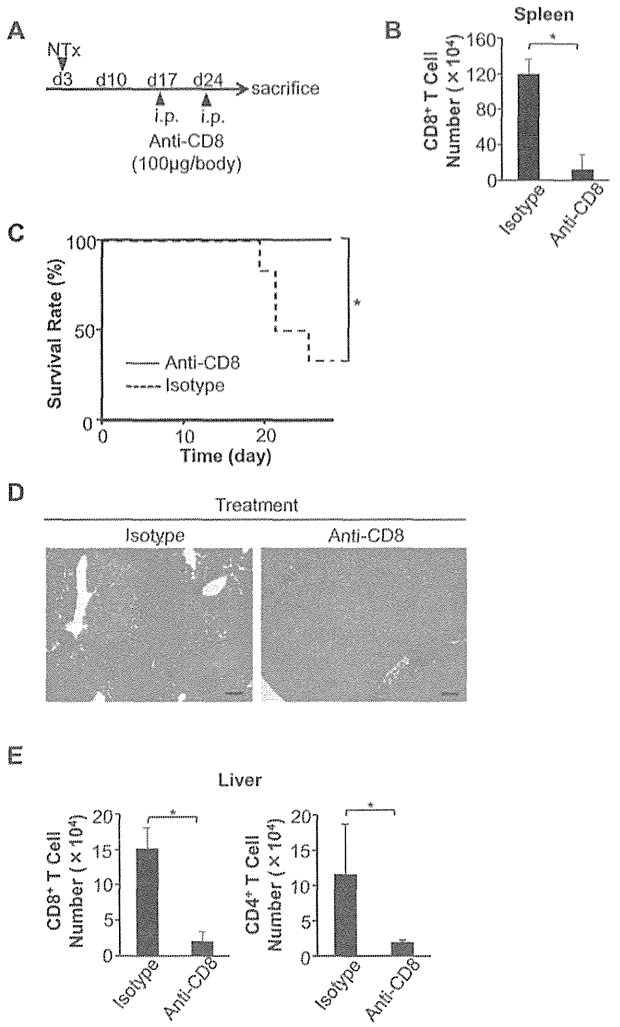

Fig. 2. Immunological and histological analysis for NTx-*PD-1*$^{-/-}$ mice injected with anti-CD8 in the progression phase of AIH. (A) NTx-*PD-1*$^{-/-}$ mice at 14 days after thymectomy were injected IP every week with 100 μg of depletion Ab to CD8 (n = 6) or the isotype control mAb (n = 6). After two injections, mice at 4 weeks of age were sacrificed. (B) Cell numbers of CD8$^+$ T cells in the spleen of NTx-*PD-1*$^{-/-}$ mice injected with indicated Abs. (C) Survival rates at 4 weeks of age. (D) Representative stainings of the liver for hematoxylin and eosin are shown. (E) Cell numbers of infiltrating T cells in liver of NTx-*PD-1*$^{-/-}$ mice injected with indicated Abs. Isolated cells were stained with FITC-anti-CD3e and APC-Cy7-anti-CD4 or APC-anti-CD8. Error bars represent standard deviation. *$P < 0.05$. FITC, fluorescein isothiocyanate; APC, allophycocyanin; Cy7, cyanine 7.

once a week with anti-CXCL9 and/or anti-CXCL10 mAbs *in vivo*. After four injections, in contrast to anti-CXCL10 injections, anti-CXCL9 injections induced a significantly higher survival rate (Fig. 4A,B). Administering anti-CXCL9 and a combination with anti-CXCL9 and anti-CXCL10, but not anti-CXCL10 alone, greatly reduced infiltration of CD4$^+$ and CD8$^+$ T cells into the liver and liver destruction at 4 weeks (Fig. 4C). These data suggest that in the progression phase of fatal AIH, the CXCR3-CXCL9 axis is crucial for migration of Th1 cells and effector CD8$^+$ T cells into the liver.

The Main Cellular Source of CXCL9 Was Hepatic Macrophages/KCs in Progression of AIH. Next, we examined which cell types express CXCL9 in the inflamed liver by IHC. We found that the majority of CXCL9-expressing cells in the inflamed liver were F4/80 antigen-positive macrophages/KCs and that CD4$^+$ and CD8$^+$ T cells were colocalized with CXCL9-expressing cells in the inflamed liver (Fig. 5A).

In AIH progression, mRNA expression of IFN-γ and TNF-α in the inflamed liver as well as serum levels of these cytokines were markedly elevated,[7-10] and IFN-γ mediated the induction of all three CXCR3 ligands (CXCL9, CXCL10, and CXCL11).[14,15] When we injected IP with 10 mg/kg of recombinant (r) IFN-γ and TNF-α in 4-week-old *PD-1*$^{-/-}$ mice, after 2 hours, IFN-γ and TNF-α significantly up-regulated mRNA expression of both CXCL9 and CXCL10 in the liver. Interestingly, we found sustained CXCL9 up-regulation by TNF-α (Fig. 5B). Indeed, neutralization of TNF-α, but not IFN-γ, suppressed hepatic CXCL9-expression in 4-week-old NTx–*PD-1*$^{-/-}$ mice (Fig. 5C).

In NTx–*PD-1*$^{-/-}$ mice, TNF-α is essential in the induction of AIH by up-regulating hepatic CCL20 expression, allowing TNF-α-producing activated T cells to migrate from the spleen into the liver.[10] In AIH progression, IHC for TNF-α revealed TNF-α production in several infiltrating cell types (Fig. 5D, left panels), suggesting that TNF-α-dependent up-regulation of CXCL9 expression may be induced by hepatic macrophages/KCs in autocrine fashion and/or by activated T cells in paracrine fashion. However, after migration of TNF-α-producing activated T cells into the liver, neutralizing serum levels of TNF-α could not suppress CXCL9 expression in the liver and serum levels of CXCL9 (Fig. 5D, right panels, and 5E). These data suggest that TNF-α secretion in autocrine and/or paracrine fashion may induce uncontrollable CXCL9 expression in progression of AIH, resulting in unsuccessful anti-TNF-α monotherapy, as previously described.[10]

Serum Levels of IL-18 Were Elevated in AIH Progression, and* In Vivo *Administration of Blocking Abs for IL-18R Signaling Suppressed Development of Fatal AIH. IL-12 is decisive in the development of Th1 subsets. A recent study showed that IL-12 can trigger naïve T cells to transitionally differentiate into T cells with features of T_{FH} and Th1 cells.[18,19] However, neutralizaing IL-12p40 did not suppress hepatic

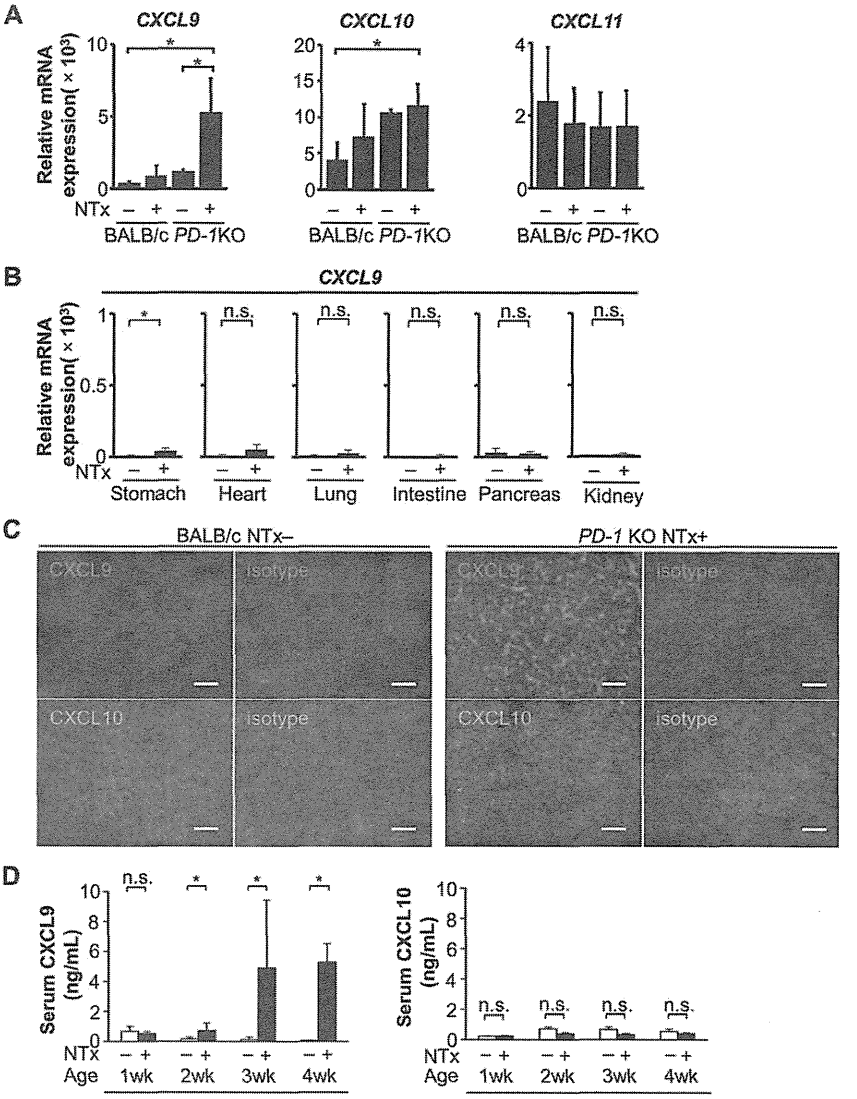

Fig. 3. Expression levels of CXCR3 ligands in NTx–*PD-1*$^{-/-}$ mice. (A) Livers from 3-week-old *PD-1*$^{-/-}$ and *PD-1*$^{+/+}$ mice with or without NTx were used for real-time qRT-PCR analyses for mRNA expressions of CXCR3 ligands CXCL9, CXCL10, and CXCL11. (B) CXCL9 mRNA expression in various organs. The stomach, heart, lung, intestine, pancreas, and kidney were from 3-week-old *PD-1*$^{-/-}$ mice with or without NTx. (C) Immunostaining with anti-CXCL9, CXCL10, or isotype controls. Livers from 3-week-old *PD-1*$^{-/-}$ and *PD-1*$^{+/+}$ mice with or without NTx were used. (D) Serum levels of CXCL9 and CXCL10 were measured by ELISA. Data are shown of sera from indicated aged *PD-1*$^{-/-}$ and *PD-1*$^{+/+}$ mice with or without NTx. Data are shown as the mean of at least 3 mice. Error bars represent standard deviation. $*P < 0.05$. n.s., not significant. Scale bars, 100 μm.

inflammation, as described previously[8] (Supporting Fig. 2). In addition, although IFN-γ has been shown to be essential for IL-12-induced Th1 differentiation,[20] neutralizing it did not suppress development of AIH.[9] These data suggest that IL-12 is not exclusively involved in differentiation into T cells with features of Th1 cells in progression of fatal AIH.

Serum levels of IL-18 are increased in patients with AIH and fatal hepatitis.[21,22] IL-18 is critical for liver injury in mice sequentially treated with *Propionibacterium acnes* and lipopolysaccharide, and for acute hepatic injury induced by concanavalin A.[23,24] When we looked at serum levels of IL-18 at 1-3 weeks of age, those of IL-18, but not IL-1β, were elevated, and IL-18 elevation gradually increased through the progression of AIH (Fig. 6A,B). IL-18 signals through the IL-18 receptor complex (IL-18R), and IL-18R contains the heterodimer IL-18Rα and IL-18Rβ subunits. The IL-18Rα subunit is responsible for extracellular binding of IL-18, whereas the IL-18Rβ subunit is nonbinding, but confers high affinity binding for the ligand, and is responsible for biological signals.[25,26] Therefore, to examine the roles of IL-18 in AIH development, NTx–*PD-1*$^{-/-}$ mice at 1 day after thymectomy were injected with IL-18Rβ mAb, which can neutralize the IL-18-mediating biological function in IL-18R-expressing cells. Administering anti-IL-18Rβ, but not anti-IL-1β, suppressed MC infiltration, including CD4$^+$ and CD8$^+$ T cells, in the liver (Fig. 6C,D), resulting in decreased serum concentrations of aspartate aminotransferase (AST) and alanine aminotransferase (ALT) and a significantly increased survival rate at 4 weeks of age (Fig. 6E,F). These data indicate that IL-18-mediated signaling is critical for development of fatal AIH in NTx–*PD-1*$^{-/-}$ mice.

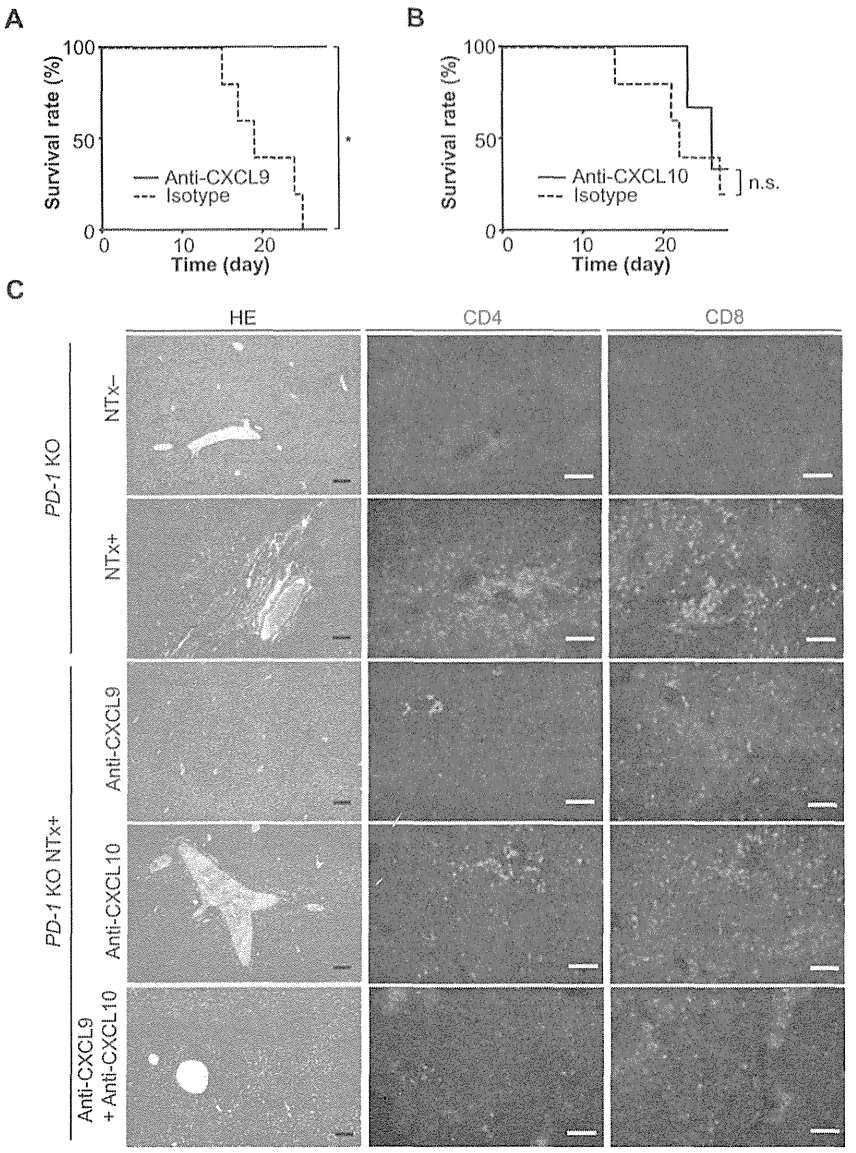

Fig. 4. Survival rate and histological analysis of the liver in NTx-*PD-1*$^{-/-}$ mice injected with neutralizing Abs for CXCR3 ligands. (A and B) NTx-*PD-1*$^{-/-}$ mice at 1 day after thymectomy were injected IP every week with 100 μg of neutralizing anti-CXCL9 (n = 5), anti-CXCL10 (n = 5), or the isotype control mAbs (n = 5). Survival rates at 4 weeks of age. (C) After four injections of anti-CXCL9, anti-CXCL10, or a combination with anti-CXCL9 and anti-CXCL10 (n = 5), mice at 4 weeks of age were sacrificed and livers were harvested. Representative stainings of the liver for hematoxylin and eosin (HE), CD4, and CD8 are shown. Upper panels are control stainings of liver in *PD-1*$^{-/-}$ mice with or without NTx. *$P < 0.05$. n.s., not significant. All scale bars, 100 μm.

IL-18 Is Mainly Produced by DCs in Spleen and Liver of NTx–PD-1$^{-/-}$ Mice. Next, we investigated how IL-18 mediates fatal AIH progression in NTx–*PD-1*$^{-/-}$ mice. We isolated MCs from liver and spleen of 2.5-week-old NTx–*PD-1*$^{-/-}$ mice and purified them to CD3$^+$CD4$^+$ T cells, CD3$^+$CD8$^+$ T cells, B220$^+$ B cells, CD11b$^+$CD11c$^-$ macrophages, CD11c$^+$ DCs, and CD3$^-$DX5$^+$ natural killer (NK) cells, then measured mRNA expression of IL-18. We found that isolated splenic and hepatic DCs increased IL-18 mRNA expression, together with up-regulated expression of NACHT, LRR, and pyrin domain-containing protein 3 (NALP3) and, to a lesser extent, IL-1β (Fig. 7A,B). In contrast, when we cultured isolated splenic DCs, IL-18, but not IL-1β, was secreted from DCs from NTx–*PD-1*$^{-/-}$ mice, but not from *PD-1*$^{-/-}$ mice (Fig. 7C and data not shown). These data suggest that in NTx–*PD-1*$^{-/-}$ mice, DCs noncanonically secrete IL-18 by activating inflammasome and promoting further differentiation of CD4$^+$ T cells into Th1 cells and CD8$^+$ T cells into effector T cells, respectively.

DCs as Well as CD4$^+$ and CD8$^+$ T Cells in Spleen and Liver Expressed IL-18R in NTx–PD-1$^{-/-}$ Mice. To evaluate whether DCs secreting IL-18 directly or indirectly modulate differentiation of T cells in NTx–*PD-1*$^{-/-}$ mice, we next examined mRNA expression of IL-18Rα on CD4$^+$ and CD8$^+$ T cells in the spleen and liver. We isolated these cells in spleen and liver of 2.5-week-old NTx–*PD-1*$^{-/-}$ mice and measured mRNA expression of IL-18Rα. We found that isolated splenic and hepatic CD4$^+$ and

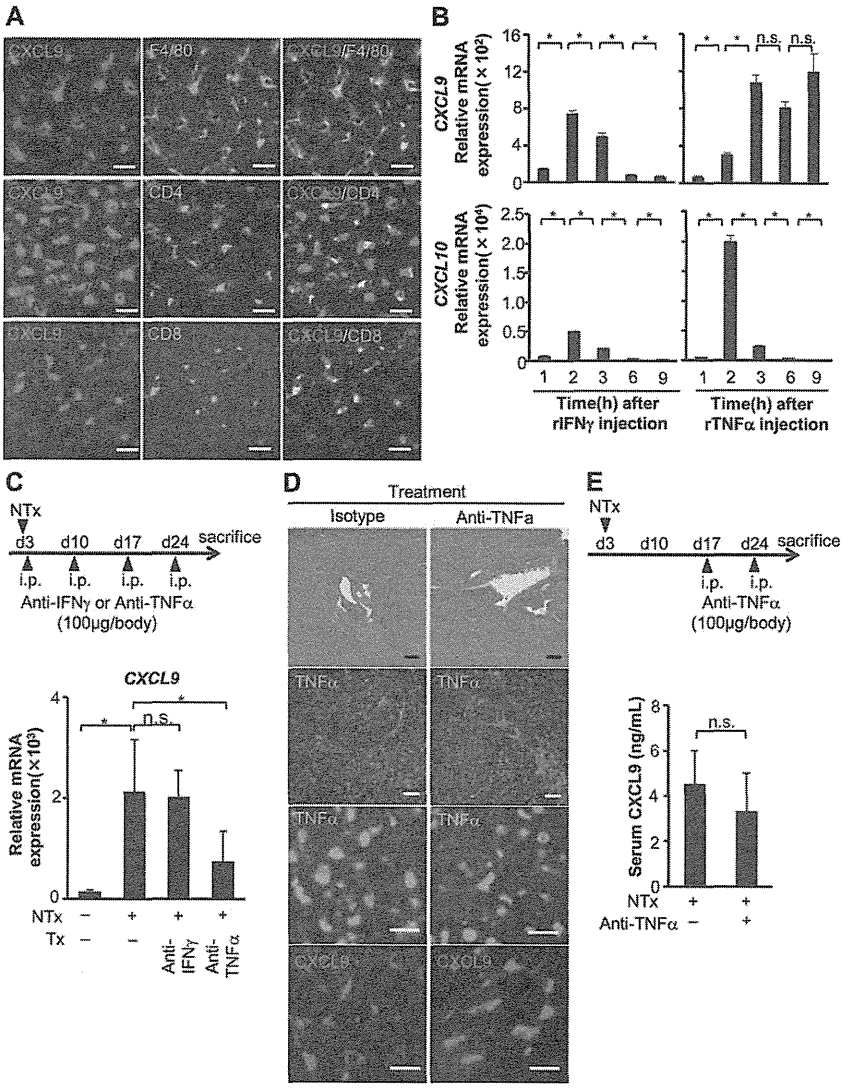

Fig. 5. Cellular source of CXCL9 and the role of cytokines in inducting CXCR3 ligands in NTx–PD-$1^{-/-}$ mice. (A) Immunostaining with anti-CXCL9, F4/80, CD4, and CD8. Livers from 3-week-old NTx–*PD-1*$^{-/-}$ mice were used. Scale bars, 20 μm. (B) Four-week-old *PD-1*$^{-/-}$ mice were injected IP with 10 μg/kg of mouse rIFN-γ or rTNF-α. Livers at the indicated time after injection were subjected to real-time qRT-PCR analyses for mRNA expressions of CXCL9 and CXCL10. (C) NTx-*PD-1*$^{-/-}$ mice at 1 day after thymectomy were injected IP every week with 100 μg of neutralizing anti-IFN-γ, anti-TNF-α, or isotype controls. After four injections, mice at 4 weeks of age were sacrificed. *PD-1*$^{-/-}$ mice without NTx at the same age were used for controls. Livers from these mice were used for real-time qRT-PCR analyses for mRNA expressions of CXCL9. (D and E) NTx-*PD-1*$^{-/-}$ mice at 14 days after thymectomy were injected IP every week with 100 μg of neutralizing anti-TNF-α or isotype control. After two injections, mice at 4 weeks of age were sacrificed. Liver stainings are shown for hematoxylin and eosin and immunostaining with anti-TNF-α. Scale bars, 50 μm (upper four panels). Immunostaining with anti-TNF-α and anti-CXCL9. Scale bars, 20 μm (lower four panels) (D). Serum levels of CXCL9 were measured by ELISA (E). Data are shown as the mean of at least three mice. Error bars represent standard deviation. *$P < 0.05$. n.s., not significant.

$CD8^+$ T cells increased IL-18Rα mRNA expression, suggesting that IL-18 can directly affect differentiation of these cells (Fig. 7D). Interestingly, isolated DCs in spleen and liver of 2.5-week-old mice expressed up-regulated expression of IL-18Rα mRNA (Fig. 7E). In addition, 4-week-old NTx–*PD-1*$^{-/-}$ mice injected with anti–IL-18Rβ mAb showed decreased serum levels of IL-18 (Fig. 7F), suggesting that IL-18 may act as an autocrine for differentiation and/or function of proinflammatory IL-18R-expressing DCs. In AIH progression, mRNA expression of IFN-γ and TNF-α in the inflamed liver as well as serum levels of these cytokines were markedly elevated,[7-10] so TNF-α could be involved in the maturation of DCs. Indeed, neutralization of TNF-α, but not IFN-γ, reduced serum levels of IL-18 (Fig. 7F), implying that TNF-α is also directly/indirectly involved in differentiation and/or function of proinflammatory IL-18R-expressing DCs.

Neutralization of IL-18R Signaling Altered Splenic T-Cell Function and Ab Production in NTx–PD-1$^{-/-}$ Mice. We found that DCs and T cells—not only in inflamed liver, but also in the spleen—expressed IL18Rα in AIH progression (Fig. 7D,E). In addition, $CD4^+$ and $CD8^+$ T cells in the spleen predominantly expressed CXCR3 (Fig. 1E).[8] We next examined whether IL-18 is involved in differentiation of splenic T cells in NTx–*PD-1*$^{-/-}$ mice. We found that injecting anti-IL-18Rβ significantly reduced the number of $CXCR3^+$ cells in $CD4^+$ T cells as well as in $CD8^+$ T cells of the spleen in 2.5-week-old NTx–*PD-1*$^{-/-}$ mice (Fig. 8A). In addition, we found that neutralizing IL-18-mediated signaling suppressed expression of T-bet, IFN-γ, TNF-α, and IL-18Rα and up-regulated expression of GATA3 in splenic $CD4^+$ T cells (Fig. 8B). Moreover, although production of total immunoglobulin (Ig) and ANA increased in NTx–*PD-1*$^{-/-}$ mice, injecting anti-IL-18Rβ reduced total Ig and ANA in

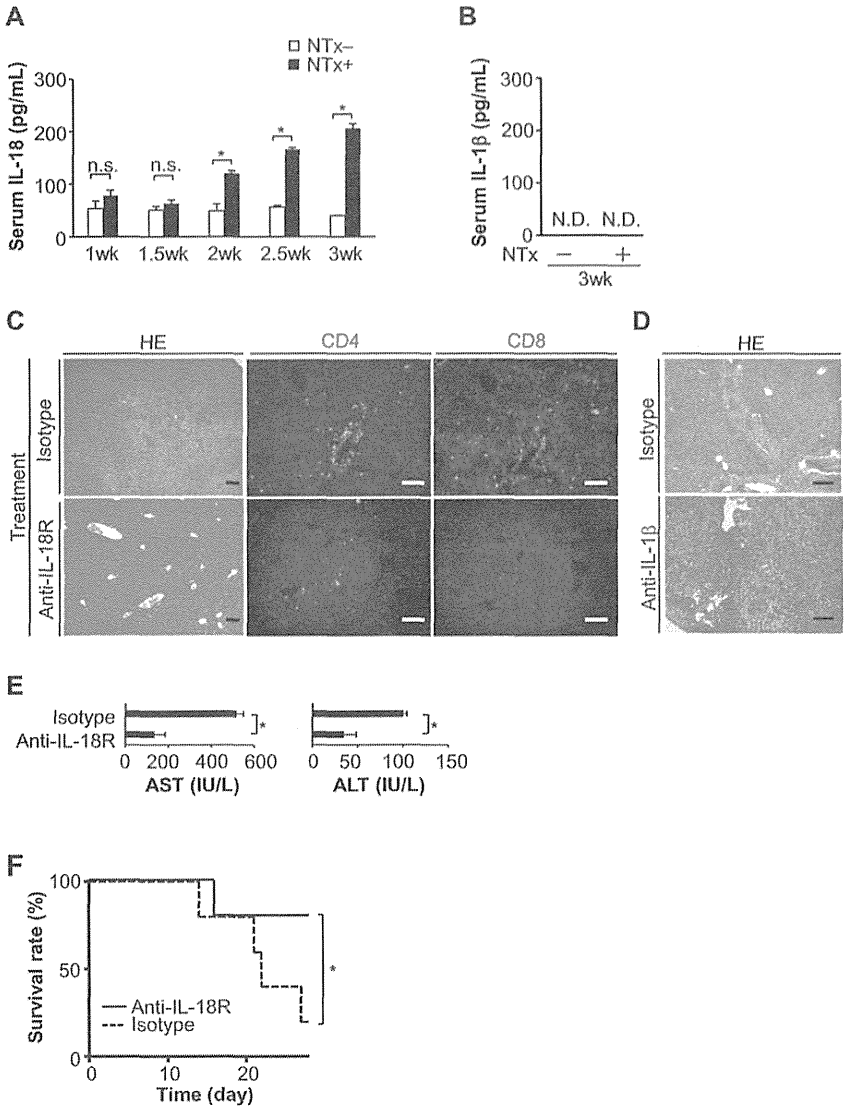

Fig. 6. Serum levels of IL-18 and IL1-β and analysis for NTx-*PD-1*$^{-/-}$ mice injected with blocking Abs for IL-18R signaling and neutralizing Abs for IL-1β. (A and B) Serum levels of IL-18 at indicated ages and IL-1β at 3 weeks of age of *PD-1*$^{-/-}$ mice with or without NTx were measured by ELISA. (C, E, and F) NTx-*PD-1*$^{-/-}$ mice at 1 day after thymectomy were injected IP every week with 100 μg of IL-18Rβ mAb (n = 10) or the isotype control mAb (n = 10). (D) NTx-*PD-1*$^{-/-}$ mice were injected with 100 μg of IL-1β mAb (n = 3) or the isotype control mAb (n = 3) as described above. After four injections, mice at 4 weeks of age were sacrificed. Stainings of the liver for hematoxylin and eosin (HE), CD4, and CD8 (C and D), serum levels of AST and ALT (E), and survival rates at 4 weeks of age (F) are shown. Data are shown as the mean of at least three mice. Error bars represent standard deviation. *$P < 0.05$. n.s., not significant. Scale bars, 100 μm.

the Th1-dependent IgG2a subclass (Supporting Fig. 3). In this mouse model, splenic CD4$^+$ T cells showing the T_{FH} cell phenotype were localized in B-cell follicles with huge GCs.[8] Although injections of anti-IL-12p40 did not significantly reduce the size of GCs in the spleen at 4 weeks, injecting anti-IL-18Rβ mAb induced enlargement of peanut agglutinin$^+$ GC in B220$^+$ follicles (Supporting Fig. 4A,B). Taken together, these data suggest that DC-derived IL-18 is involved in differentiation of CD4$^+$T cells into Th1 cells and CD8$^+$ T cells into effector T cells, respectively, in spleen of NTx–*PD-1*$^{-/-}$ mice.

Discussion

In this study, using our fatal AIH model, we examined molecules key to the triggering of fatal progression of AIH. We found that in the progression, CXCR3 expressing Th1 cells and CD8$^+$ effector T cells infiltrated the liver, with CD8$^+$ effector T cells triggering the fatal destruction of the liver, that hepatic macrophages/KCs producing CXCL9 is critical for migration of these T cells, and that DC-derived IL-18 is critical for differentiation of Th1 cells and CD8$^+$ effector T cells (Fig. 8C).

We previously reported that in the induction phase of AIH in 2-week-old NTx–*PD-1*$^{-/-}$ mice, IL-21-producing splenic T_{FH} cells directly migrated into the liver through the CCR6-CCL20 axis, triggering AIH.[8] In contrast, we showed here that in severely inflamed livers in 3-week-old NTx–*PD-1*$^{-/-}$ mice, DC-derived IL-18 mediates differentiation of Th1 cells and CD8$^+$ effector T cells, and the CXCR3-CXCL9 axis triggers the migration of these T cells, resulting in fatal AIH progression. Therefore, in the

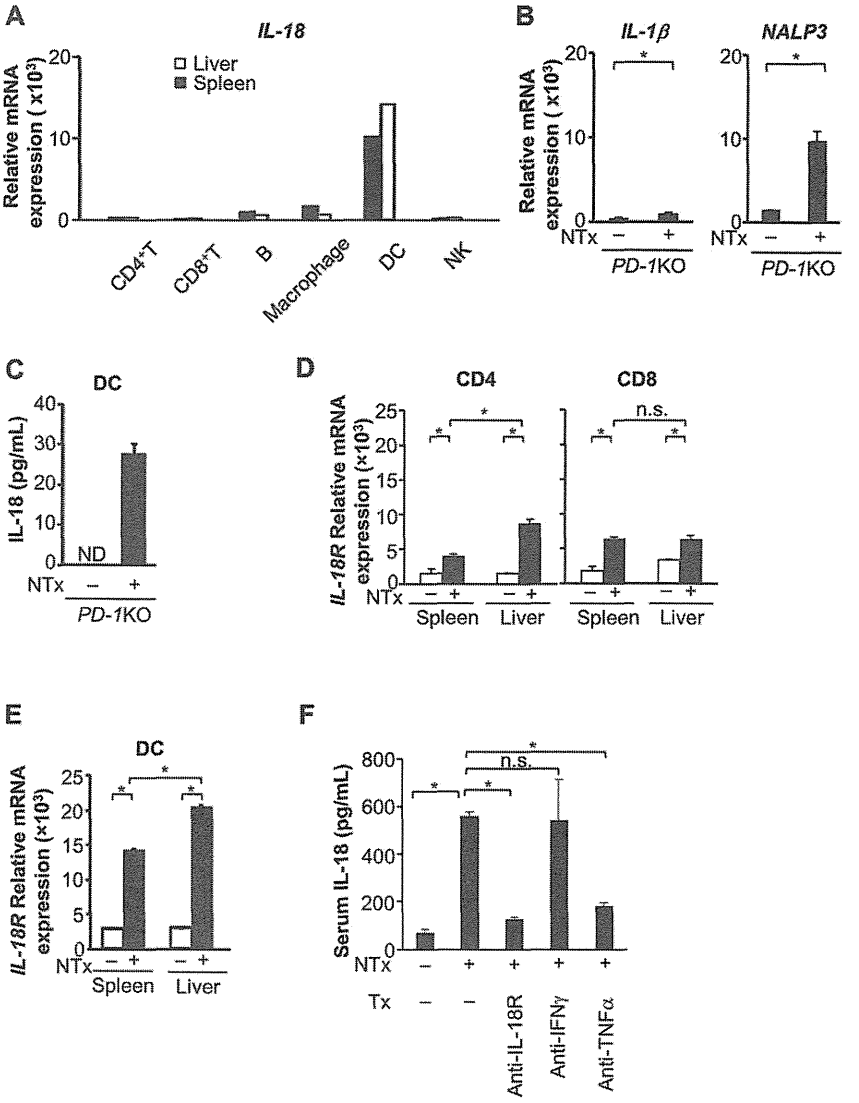

Fig. 7. Expression levels of IL-18, IL-1β, NALP3, and IL-18Rα in AIH-bearing 2.5-week-old NTx-*PD-1*$^{-/-}$ mice. (A) Expression levels of mRNA encoding IL-18 of CD3$^+$CD4$^+$ T cells, CD3$^+$CD8$^+$ T cells, B220$^+$ B cells, CD11b$^+$CD11c$^-$ macrophages, CD11c$^+$ DCs, and CD3$^-$DX5$^+$ NK cells in spleen and liver of 2.5-week-old NTx-*PD-1*$^{-/-}$ mice. Data represent one of three independent experiments. (B) Expression levels of mRNA encoding IL-1β and NALP3 of CD11c$^+$ DCs in spleen of 2.5-week-old NTx-PD-1$^{-/-}$ mice. (C) Concentration of IL-18 in DC culture supernatants measured by ELISA. CD11c$^+$ DCs were isolated from spleen in *PD-1*$^{-/-}$ mice with or without NTx and DCs were cultured for 24 hours. Data are shown as the mean of triplicates. (D and E) Expression levels of mRNA encoding IL-18Rα of CD3$^+$CD4$^+$ and CD3$^+$CD8$^+$ T cells (D) and CD11c$^+$ DCs (E) in spleen and liver of 2.5-week-old NTx-*PD-1*$^{-/-}$ mice. (F) Serum levels of IL-18 were measured by ELISA. NTx-*PD-1*$^{-/-}$ mice at 1 day after thymectomy were injected IP every week with 100 μg of neutralizing anti-IL-18Rβ, anti-IFN, or anti-TNF-α. After four injections, mice at 4 weeks of age were sacrificed. Data are shown of sera from *PD-1*$^{-/-}$ mice of 4 weeks of age with indicated condition. Data are shown as the mean of at least three mice. Error bars represent standard deviation. *$P < 0.05$. n.s., not significant; ND, not detected.

development of fatal AIH in our model, different types of T cells are critically involved at different time points in the induction and fatal progression of AIH. This involvement has also been reported in experimental autoimmune encephalomyelitis (EAE), a CD4$^+$ T-cell-mediated disease of the central nervous system (CNS).[27] In EAE, Th17 cells migrate through the CCR6-CCL20 axis, triggering inflammation in the induction phase, whereas Th1 cells are mainly involved in inflamed lesions in the CNS during active progression.[27] In addition, a recent study reported that T_{FH}-like cells were transiently generated during IL-12-mediating Th1 cell differentiation. In mice infected with *Toxoplasma gondii*, an obligate intracellular parasite, T_{FH}-like cells were generated 7 days after infection, the proportion of T_{FH}-like cells declined, and IFN-γ-producing Th1 cells increased at day 15.[19]

In this study, we showed that DC-derived IL-18 is critical for differentiation of Th1 cells and CD8$^+$ effector T cells in AIH progression. IL-18 is known to be produced by various types of immune cells and epithelial cells.[25,26] In humans, IL-18 produced by DCs promotes Th1 induction.[28] IL-18 stimulates Th1-mediated immune responses and activates Th1 cells, which highly express functional IL-18 receptor, producing large amounts of IFN-γ.[25,26] In addition, in an atopic dermatitis mouse model, IL-18 could induce differentiation of Th1-like cells that expressed IFN-γ and CXCR3.[29] In humans, IL-18 has been shown to be involved in disease processes associated with excessive Th1 responses in several inflammatory diseases, including autoimmune diseases.[30-32] Patients with acute hepatitis, chronic liver disease, fulminant hepatitis, primary biliary cirrhosis, or AIH all show elevated serum levels of IL-18,[21,22] which correlates with disease severity.[33,34]

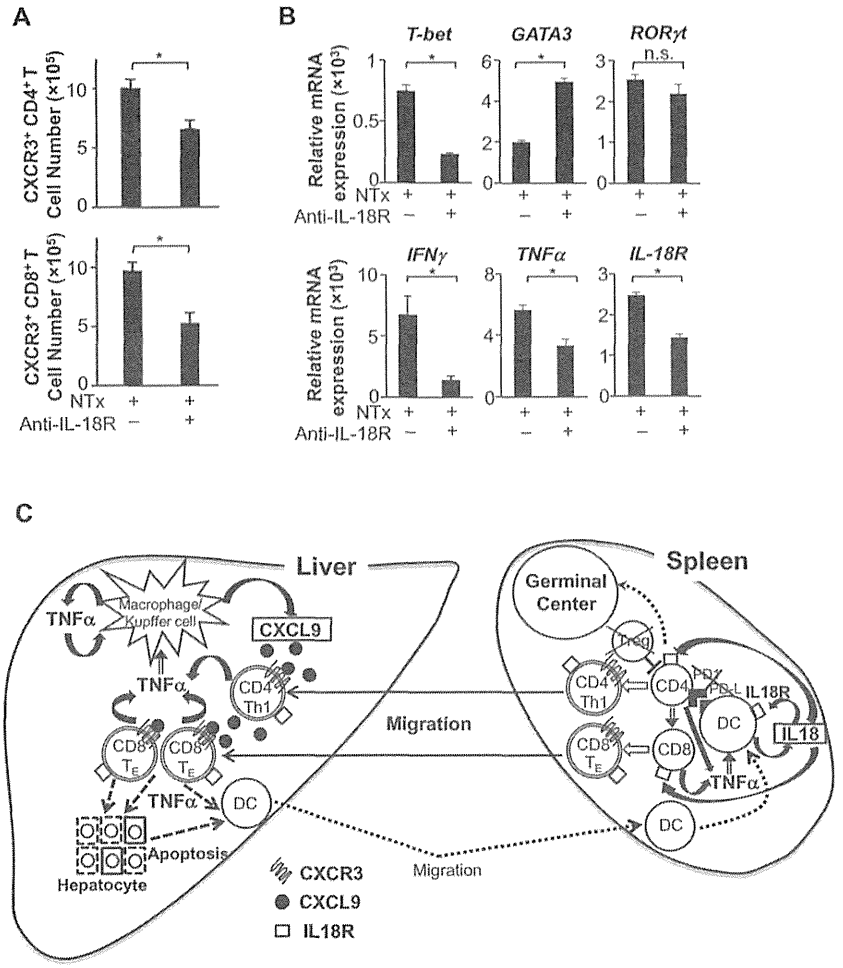

Fig. 8. Immunological and RT-PCR analysis for NTx-*PD-1*$^{-/-}$ mice injected with blocking Abs for IL-18R signaling and the model of pathological mechanisms in the progression phase of AIH in NTx-*PD-1*$^{-/-}$ mice. (A and B) NTx-*PD-1*$^{-/-}$ mice at 1 day after thymectomy were injected with IL-18Rβ mAb. (A) After four injections, mice at 4 weeks of age were sacrificed as described in Fig. 6. Cell numbers of CXCR3^{+} cells in CD4^{+} and CD8^{+} T cells in the spleen. Data are shown as the mean of at least 3 mice. (B) After three injections, mice at 3 weeks of age were sacrificed, and CD4^{+} T cells were isolated from spleens. Expression levels of mRNA encoding T-bet, GATA-3, ROR-γt, IFN-γ, TNF-α, and IL-18Rα were measured. Data are shown as the mean of triplicates. Error bars represent standard deviation. *$P < 0.05$. n.s., not significant. (C) Model of mechanistic links of cytokines and chemokines in the progression phase of NTx-*PD-1*$^{-/-}$ mice. In the progression, DC-derived IL-18 is critical for differentiation of CXCR3-expressing Th1 cells and CD8^{+} effector T cells (T_E). CXCL9 production by hepatic macrophages/KCs triggers migration of these T cells into the liver. CXCR3-expressing T_E and, to a lesser extent, Th1 infiltrate the liver and T_E trigger the fatal destruction of the liver. ROR-γt, retinoid-related orphan receptor-gamma t.

We found that splenic and hepatic DCs increased IL-18 mRNA expression, together with up-regulated expression of NALP3 and, to a lesser extent, IL-1β. However, DCs only secreted IL-18 and induced elevation of serum levels of IL-18. Indeed, administering anti-IL-18Rβ, but not anti-IL-1β, suppressed fatal AIH. After inflammasome activation by NALP3 occurs in the cells, inactive pro-caspase-1 is activated into active caspase-1. Subsequent to cleavage by active caspase-1, mature IL-18 as wells as IL-1β can be secreted from cells.[35] These canonical IL-1β and IL-18 secretions by inflammasome activation are involved in acetaminophen-induced liver injury.[36] However, several recent studies suggest that secretion of IL-18, but not IL-1β, by activation of inflammasome and caspase-1 can be orchestrated by several distinct regulatory mechanisms.[37-39] Thus, in NTx–*PD-1*$^{-/-}$ mice, distinct licensing of IL-1β and IL-18 secretion may be involved in the noncanonical secretion of IL-18 by activation of inflammasome.

Because TNF-α can directly induce maturation of DCs, TNF-α and IL-18 may directly induce inflammasome up-regulation and skew toward IL-18 production through repression of IL-1β transcript, but up-regulation of IL-18 transcript. On the other hand, TNF-α directly and indirectly induces cell death of hepatocytes[40] and free DNA released from apoptotic hepatocytes can activate Toll-like receptor 9, triggering a signaling cascade to induce pro-IL-1β and pro-IL-18.[36] Therefore, TNF-α may induce apoptosis of hepatocytes, triggering canonical IL-18 production initially. However, IL-18 may act as an autocrine for skewing prolonged IL-18 secretion in DCs.

Although first described as IFN-γ-inducing factor, IL-18 may not make a major contribution to elevated serum levels of IFN-γ in AIH progression. In contrast to IL-18, serum levels of IFN-γ reached the maximal level at 1 week of age before AIH development; the elevated serum level of IFN-γ gradually decreased during AIH progression.[9] Indeed, IFN-γ was dispensable for up-regulating CXCL9 in the liver. Neutralizing IFN-γ did not prevent development of AIH and induced increased T-cell proliferation in the spleen and liver, resulting in exacerbated T-cell infiltration in AIH.[9] So, although

IFN-γ generally acts as a critical proinflammatory mediator, it exerts regulatory functions to limit tissue damage associated with inflammation of AIH in progression.

We showed here that migration of exclusively CXCR3-expressing T cells was triggered by hepatic macrophages/KCs producing one CXCR3 ligand, CXCL9. Although CXCL9, CXCL10, and CXCL11 can bind to the common receptor, CXCR3, differences have been reported in the kinetics and the tissue/cell-type expression patterns of these three chemokine genes and their proteins during infection or inflammatory responses.[41-44] Studies using CXCL9- or CXCL10-deficient mice have shown the nonredundant function of these chemokines in various immunoinflammatory settings, including a hepatitis B virus transgenic mouse model and a liver injury model.[41-44]

In this study, we showed that CXCL9-expressing cells are macrophages/KCs in AIH progression. Although recombinant (r)IFN-γ and rTNF-α up-regulated hepatic CXCL9 expression, anti-IFN-γ did not suppress hepatic CXCL9 up-regulation. In NTx–*PD-1*$^{-/-}$ mice, cell types responsible for secreting CXCR3 ligands in various organs may exhibit a refractory response to constitutively elevated serum IFN-γ. In addition, TNF-α secreted in autocrine and in paracrine fashion by activated T cells may induce uncontrollable CXCL9 expression in AIH progression. Therefore, anti-TNF-α monotherapy may not significantly prevent fatal AIH in mice.

In conclusion, we have identified the pivotal role of the IL-18 and the CXCR3-CXCL9 axis in fatal progression of AIH, implying that blocking these systems may have clinical potential for protecting against fatal progression of this disease.

Acknowledgment: The authors thank Dr. Taku Okazaki and Tasuku Honjo for providing PD-1-deficient mice, Dr. Dovie Wylie for assistance in preparation of the manuscript, Ms. Chigusa Tanaka for her excellent technical assistance, and Drs. Shuh Narumiya, Nagahiro Minato, Shimon Sakaguchi, Takeshi Watanabe, and Ichiro Aramori for their critical discussion and suggestions.

References

1. Nikias GA, Batts KP, Czaja AJ. The nature and prognostic implications of autoimmune hepatitis with an acute presentation. J Hepatol 1994; 21:866-871.
2. Yamamoto K, Miyake Y, Ohira H, Suzuki Y, Zeniya M, Onji M, et al. Prognosis of autoimmune hepatitis showing acute presentation. Hepatol Res 2013;43:630-638.
3. Soloway RD, Summerskill WH, Baggenstoss AH, Geall MG, Gitnick GL, Elveback IR, et al. Clinical, biochemical, and histological remission of severe chronic active liver disease: a controlled study of treatments and early prognosis. Gastroenterology 1972;63:820-833.
4. Verma S, Torbenson M, Thuluvath PJ. The impact of ethnicity on the natural history of autoimmune hepatitis. HEPATOLOGY 2007;46:1828-1835.
5. Verma S, Maheshwari A, Thuluvath P. Liver failure as initial presentation of autoimmune hepatitis: clinical characteristics, predictors of response to steroid therapy, and outcomes. HEPATOLOGY 2009;49:1396-1397.
6. Manns MP, Czaja AJ, Gorham JD, Krawitt EL, Mieli-Vergani G, Vergani D, et al. Diagnosis and management of autoimmune hepatitis. HEPATOLOGY 2010;51:2193-2213.
7. Kido M, Watanabe N, Okazaki T, Akamatsu T, Tanaka J, Saga K, et al. Fatal autoimmune hepatitis induced by concurrent loss of naturally arising regulatory T cells and PD-1-mediated signaling. Gastroenterology 2008:135:1333-1343.
8. Aoki N, Kido M, Iwamoto S, Nishiura H, Maruoka R, Tanaka J, et al. Dysregulated generation of follicular helper T cells in the spleen triggers fatal autoimmune hepatitis in mice. Gastroenterology 2011;140: 1322-1333.
9. Iwamoto S, Kido M, Aoki N, Nishiura H, Maruoka R, Ikeda A, et al. IFN-γ is reciprocally involved in the concurrent development of organ-specific autoimmunity in the liver and stomach. Autoimmunity 2012; 45:186-198.
10. Iwamoto S, Kido M, Aoki N, Nishiura H, Maruoka R, Ikeda A, et al. TNF-α is essential in the induction of fatal autoimmune hepatitis in mice through upregulation of hepatic CCL20 expression. Clin Immunol 2013;146:15-25.
11. Maruoka R, Aoki N, Kido M, Iwamoto S, Nishiura H, Ikeda A, et al. Splenectomy prolongs the effects of corticosteroids in mouse models of autoimmune hepatitis. Gastroenterology 2013;145:209-220.
12. King C. New insights into the differentiation and function of T follicular helper cells. Nat Rev Immunol 2009;9:757-766.
13. Nishimura H, Okazaki T, Tanaka Y, Nakatani K, Hara M, Matsumori A, et al. Autoimmune dilated cardiomyopathy in PD-1 receptor-deficient mice. Science 2001;291:319-322.
14. Liu L, Callahan MK, Huang D, Ransohoff RM. Chemokine receptor CXCR3: an unexpected enigma. Curr Top Dev Biol 2005;68: 149-181.
15. Groom JR, Luster AD. CXCR3 in T cell function. Exp Cell Res 2011; 317:620-631.
16. Lacotte S, Brun S, Muller S, Dumortier H. CXCR3, inflammation, and autoimmune diseases. Ann N Y Acad Sci 2009;1173:310-317.
17. Lee EY, Lee ZH, Song YW. CXCL10 and autoimmune diseases. Autoimmun Rev 2009;8:379-383.
18. Szabo SJ, Sullivan BM, Peng SL, Glimcher LH. Molecular mechanisms regulating Th1 immune responses. Annu Rev Immunol 2003;21: 713-758.
19. Nakayamada S, Kanno Y, Takahashi H, Jankovic D, Lu KT, Johnson TA, et al. Early Th1 cell differentiation is marked by a Tfh cell-like transition. Immunity 2011;35:919-931.
20. Wenner CA, Güler ML, Macatonia SE, O'Garra A, Murphy KM. Roles of IFN-γ and IFN-γ in IL-12-induced T helper cell-1 development. J Immunol 1996;156:1442-1447.
21. Yamano T, Higashi T, Nouso K, Nakatsukasa H, Kariyama K, Yumoto E, et al. Serum interferon-gamma-inducing factor/IL-18 levels in primary biliary cirrhosis. Clin Exp Immunol 2000;122:227-231.
22. Yumoto E, Higashi T, Nouso K, Nakatsukasa H, Fujiwara K, Hanafusa T, et al. Serum gamma-interferon-inducing factor (IL-18) and IL-10 levels in patients with acute hepatitis and fulminant hepatic failure. J Gastroenterol Hepatol 2002;17:285-294.
23. Tsutsui H, Kayagaki N, Kuida K, Nakano H, Hayashi N, Takeda K, et al. Caspase-1-independent, Fas/Fas ligand-mediated IL-18 secretion from macrophages causes acute liver injury in mice. Immunity 1999; 11:359-367.
24. Faggioni R, Jones-Carson J, Reed DA, Dinarello CA, Feingold KR, Grunfeld C, et al. Leptin-deficient (ob/ob) mice are protected from T cell-mediated hepatotoxicity: role of tumor necrosis factor α and IL-18. Proc Natl Acad Sci U S A 2000;97:2367-2372.

25. Reddy P. Interleukin-18: recent advances. Curr Opin Hematol 2004; 11:405-410.
26. Arend WP, Palmer G, Gabay C. IL-1, IL-18, and IL-33 families of cytokines. Immunol Rev 2008;223:20-38.
27. Reboldi A, Coisne C, Baumjohann D, Benvenuto F, Bottinelli D, Lira S, et al. C-C chemokine receptor 6-regulated entry of TH-17 cells into the CNS through the choroid plexus is required for the initiation of EAE. Nat Immunol 2009;10:514-523.
28. Kaser A, Kaser S, Kaneider NC, Enrich B, Wiedermann CJ, Tilg H. Interleukin-18 attracts plasmacytoid dendritic cells (DC2s) and promotes Th1 induction by DC2s through IL-18 receptor expression. Blood 2004;103:648-655.
29. Terada M, Tsutsui H, Imai Y, Yasuda K, Mizutani H, Yamanishi K, et al. Contribution of IL-18 to atopic-dermatitis-like skin inflammation induced by Staphylococcus aureus product in mice. Proc Natl Acad Sci U S A 2006;103:8816-8821.
30. Calvani N, Tucci M, Richards HB, Tartaglia P, Silvestris F. Th1 cytokines in the pathogenesis of lupus nephritis: the role of IL-18. Autoimmun Rev 2005;4:542-548.
31. Dinarello CA. Interleukin-18 and the pathogenesis of inflammatory diseases. Semin Nephrol 2007;27:98-114.
32. Wittmann M, Macdonald A, Renne J. IL-18 and skin inflammation. Autoimmun Rev 2009;9:45-48.
33. Sharma A, Chakraborti A, Das A, Dhiman RK, Chawla Y. Elevation of interleukin-18 in chronic hepatitis C: implications for hepatitis C virus pathogenesis. Immunology 2009;128:e514-e522.
34. Ludwiczek O, Kaser A, Novick D, Dinarello CA, Rubinstein M, Vogel W, et al. Plasma levels of interleukin-18 and interleukin-18 binding protein are elevated in patients with chronic liver disease. J Clin Immunol 2002;22:331-337.
35. Franchi L, Eigenbrod T, Muñoz-Planillo R, Nuñez G. The inflammasome: a caspase-1-activation platform that regulates immune responses and disease pathogenesis. Nat Immunol 2009;10:241-247.
36. Imaeda AB, Watanabe A, Sohail MA, Mahmood S, Mohamadnejad M, Sutterwala FS, et al. Acetaminophen-induced hepatotoxicity in mice is dependent on Tlr9 and the Nalp3 inflammasome. J Clin Invest. 2009; 119:305-314.
37. Kahlenberg JM, Thacker SG, Berthier CC, Cohen CD, Kretzler M, Kaplan MJ. Inflammasome activation of IL-18 results in endothelial progenitor cell dysfunction in systemic lupus erythematosus. J Immunol 2011;187:6143-6156.
38. Schmidt RL, Lenz LL. Distinct licensing of IL-18 and IL-1β secretion in response to NLRP3 inflammasome activation. PLoS One 2012;7: e45186.
39. Jitprasertwong P, Jaedicke KM, Nile CJ, Preshaw PM, Taylor JJ. Leptin enhances the secretion of interleukin (IL)-18, but not IL-1β, from human monocytes via activation of caspase-1. Cytokine 2014;65:222-230.
40. Schwabe RF, Brenner DA. Mechanisms of liver injury. I. TNF-alpha-induced liver injury: role of IKK, JNK, and ROS pathways. Am J Physiol Gastrointest Liver Physiol 2006;290:G583-G589.
41. Mach F, Sauty A, Iarossi AS, Sukhova GK, Neote K, Libby P, et al. Differential expression of three T lymphocyte-activating CXC chemokines by human atheroma-associated cells. J Clin Invest 1999;104: 1041-1050.
42. Kakimi K, Lane TE, Wieland S, Asensio VC, Campbell IL, Chisari FV, et al. Blocking chemokine responsive to γ-2/interferon (IFN)-γ inducible protein and monokine induced by IFN-γ activity in vivo reduces the pathogenetic but not the antiviral potential of hepatitis B virus-specific cytotoxic T lymphocytes. J Exp Med 2001;194:1755-1766.
43. Zhai Y, Shen XD, Gao F, Zhao A, Freitas MC, Lassman C, et al. CXCL10 regulates liver innate immune response against ischemia and reperfusion injury. HEPATOLOGY 2008;47:207-214.
44. Menke J, Zeller GC, Kikawada E, Means TK, Huang XR, Lan HY, et al. CXCL9, but not CXCL10, promotes CXCR3-dependent immune-mediated kidney disease. J Am Soc Nephrol 2008;19:1177-1189.

Supporting Information

Additional Supporting Information may be found in the online version of this article at the publisher's website.

Japan College of Rheumatology
MODERN RHEUMATOLOGY

http://informahealthcare.com/mor
ISSN 1439-7595 (print), 1439-7609 (online)

Mod Rheumatol, 2014; Early Online: 1–6

DOI: 10.3109/14397595.2014.990674

informa
healthcare

ORIGINAL ARTICLE

Total lesion glycolysis as an IgG4-related disease activity marker

Yoshinari Nakatsuka[1], Tomohiro Handa[1], Yuji Nakamoto[2], Tomomi Nobashi[2], Hajime Yoshihuji[3], Kiminobu Tanizawa[4], Kohei Ikezoe[1], Akihiko Sokai[1], Takeshi Kubo[2], Toyohiro Hirai[1], Kazuo Chin[4], Kaori Togashi[2], Tsuneyo Mimori[3], and Michiaki Mishima[1]

[1]*Department of Respiratory Medicine, Graduate School of Medicine, Kyoto University, Kyoto, Japan,* [2]*Department of Diagnostic Imaging and Nuclear Medicine, Graduate School of Medicine, Kyoto University, Kyoto, Japan,* [3]*Department of Rheumatology and Clinical Immunology, Graduate School of Medicine, Kyoto University, Kyoto, Japan, and* [4]*Department of Respiratory Care and Sleep Control Medicine, Graduate School of Medicine, Kyoto University, Japan*

Abstract

Objectives. 2-[18F]-fluoro-2-deoxy-D-glucose-positron emission tomography/computed tomography (FDG-PET/CT) was reported to be useful for monitoring immunoglobulin G4-related disease (IgG4-RD); however, a quantitative FDG-PET/CT analysis such as total lesion glycolysis (TLG) has not yet been conducted. This study aimed to investigate whether TLG would correlate with serum markers in IgG4-RD, and the utility of TLG for disease monitoring.

Methods. This retrospective study included 17 patients (12 men; median age, 62 years) who were followed up at Kyoto University Hospital and underwent FDG-PET/CT from April 2009 to November 2013. TLG was calculated for the involved lesions. Correlations between serum markers [IgG4, soluble IL-2 receptor (sIL-2R), lactate dehydrogenase (LDH), and C-reactive protein (CRP)] and TLG concomitant with FDG-PET/CT scans were investigated. Serial changes in TLG were assessed in patients who underwent follow-up FDG-PET/CT ($n = 6$).

Results. The calculated median (IQL) TLG value was 154.8 (63.7–324.4). A significant correlation was found between the sIL-2R level and TLG ($P = 0.001$, rs = 0.763). In contrast, no correlations were found between the IgG4, LDH, or CRP levels and TLG. Increased or decreased TLG corresponded with clinical disease improvement or worsening.

Conclusions. TLG correlated significantly with the serum sIL-2R level and may be useful for disease monitoring in IgG4-RD.

Keywords

FDG-PET, IgG4-related disease, Soluble IL-2 receptor, Total lesion glycolysis

History

Received 7 August 2014
Accepted 19 November 2014
Published online 29 December 2014

Introduction

Immunoglobulin G4-related disease (IgG4-RD) is a multiorgan disease that is histologically characterized by the marked infiltration of IgG4-positive plasma cells into affected organs and elevated serum IgG4 levels [1,2]. Commonly affected sites include the pancreas (autoimmune pancreatitis), salivary glands (Mikulicz disease), retroperitoneal space (retroperitoneal fibrosis), lymph nodes, and lungs [3]. To date, there are no established clinical indices for evaluating IgG4-RD activity [4].

2-[18F]-fluoro-2-deoxy-D-glucose-positron emission tomography/computed tomography (FDG-PET/CT) is a commonly used diagnostic tool for malignant diseases. FDG-PET/CT has been reported to be useful for lesion detection and disease activity evaluations in IgG4-RD cases [4,5]. A major advantage of FDG-PET/CT is that it provides quantitative data regarding lesion metabolic activity on a whole-body scale [5]. Total lesion glycolysis (TLG) is a recently proposed FDG uptake parameter; this parameter is calculated as the mean standardized uptake value (SUVmean) × the metabolic tumor volume (MTV). TLG reflects the total FDG uptake in the lesion, and a summation of TLG value from each lesion can indicate global metabolic disease activity in patients with multiorgan disorder [6]. However, there is no paper that investigated TLG in IgG4-RD; therefore, it is unknown in IgG4-RD patients whether TLG correlates serum markers of inflammations and whether serial change of TLG coincides with clinical course.

In the present study, to evaluate the utility of TLG for assessing IgG4-RD activity, we calculated the TLG values of IgG4-RD patients and determined whether these values correlated with serum levels of inflammatory biomarkers. Additionally, we compared changes in TLG with clinical courses of patients who underwent serial FDG-PET/CT studies.

Materials and methods

Study subjects

This retrospective study included 17 patients (12 men and 5 women) who were diagnosed with definite IgG4-RD at Kyoto University Hospital and underwent FDG-PET/CT before the initiation of immunosuppressive therapy during the period from April 2009 to November 2013. Seven of these cases were recurrent for which corticosteroid or immunosuppressive therapy had not been administered within 6 months prior to the FDG-PET/CT scan. The diagnoses were based on the criteria proposed by Umehara et al. [1]. Only the definite cases were included which fulfilled all of the following criteria: characteristic lesion

Correspondence to: Tomohiro Handa, MD, PhD, Department of Respiratory Medicine Graduate School of Medicine, Kyoto University, 54 Shogoin Kawaharacho, Sakyo-ku, Kyoto 606-8507. Tel: + 81-75-751-3830. Fax: + 81-75-751-4643. E-mail: hanta@kuhp.kyoto-u.ac.jp

distribution, an elevated serum IgG4 level (> 135 mg/dL), and histopathological findings compatible with IgG4-RD. The median (interquartile) age at the first test was 62 (range, 58 – 73) years. Patients initially underwent FDG-PET/CT because of suspected malignant disease (e.g., malignant lymphoma) and were ultimately diagnosed with IgG4-RD. Patients were excluded from study if FDG-PET/CT had been performed at an institute other than Kyoto University Hospital, or if corticosteroid or another immunosuppressive therapy had been administered at the time of the initial FDG-PET/CT scan. Patients with active malignant diseases were excluded; however, three cases with histories of malignancies within 5 years prior to FDG-PET/CT (thyroid cancer, colon cancer, and double lung and breast cancer) were included because in each case, radical treatment had been performed and malignant recurrence had been clinically excluded.

Twelve patients were symptomatic, and salivary gland swelling and hydronephrosis-related symptoms such as abdominal pain were comparatively common, whereas five cases did not complain of any symptoms. Comorbidities included diabetes mellitus in three cases, bronchial asthma in two and Grave's disease in two; in all cases the comorbid diseases were well controlled. The number of involved organs varied with a maximum of eight affected organs. Thirteen patients received corticosteroid therapy at a median (interquartile) dose of 35 (31.3 – 36) mg/day upon conversion to prednisolone. Patient characteristics are summarized in Table 1.

The Kyoto University Hospital Institutional Review Board approved this study (E201).

FDG-PET/CT imaging

PET/CT scan was performed on a combined PET/CT scanner (Discovery ST Elite; GE Healthcare, Little Chalfont, UK). Patients fasted for at least 4 h before the study and after the plasma glucose level was confirmed to be < 150 mg/dL, each patient received an intravenous administration of a standard dose of 3.7MBq/kg of FDG. Approximately 60 min after the injection, a low-dose CT scan and successive PET scan covering the levels from the upper thigh to the skull was performed while the patient maintained shallow breathing. In this PET/CT scan system, CT and PET images were coregistered and the CT data were used for attenuation correction. These images were reconstructed using the VUE Point Plus 3-dimensional iterative reconstruction algorithm.

Table 1. Patient characteristics.

	All patients, N = 17
Sex, male/female	12/5
Age, years	66 (57–73)
Symptoms	
Symptomatic*	12
Hydronephrosis-related symptoms	6
Salivary gland swelling	2
Exophthalmos	3
Dry mouth or dry eye	2
Asymptomatic	5
Comorbidities	
Hypertension	5
Diabetes	3
Asthma	2
Grave's disease	2
Angina pectoris	2
Number of involved organs	
1	4
2	4
3	3
4	4
5 ≦	2
Serum IgG, mg/dl	2179 (1820–2761)
Serum IgE, mg/dl	740 (400–1100)
Corticosteroid therapy	13
Initial corticosteroid dose, mg/day	35 (32.3–36)

Values are presented as medians (interquartile ranges) or numbers.
MTV metabolic tumor volume, *TLG* total lesion glycolysis, *sIL-2R* soluble interleukin- 2 receptor, *IgG4* immunoglobulin G4.
*One patient complained of abdominal pain due to hydronephrosis as well as dry mouth and was counted separately.

Image interpretation

All images were reviewed for consensus by two observers (one nuclear medicine physician and one pulmonary physician). FDG accumulation was assessed on a workstation (Advantage Workstation, GE Healthcare) by calculating the standardized uptake value (SUV) in the regions of interest. SUV was calculated using the following formula: SUV = Cdc/(Di/W), where Cdc is the decay-corrected tracer tissue concentration (in Bq/g); Di is the injected dose (in Bq); and W is the patient's body weight (in g). Abnormal FDG uptake was identified based on a visual comparison of FDG uptake between the background organ and target site. All sites with abnormal FDG uptake were considered approximate foci of IgG4-RD lesions, although pathological analysis was not available for all sites. Next, we manually drew a 3D cuboid contour surrounding the abnormal uptake site. Within this contour, the voxels with SUV equal to or greater than the cut-off value were automatically extracted and defined as the optimal lesion border (Figure 1). In the present study, the cut-off value was fixed at 2.5 in accordance with previous reports [7–10]. The lesion volume was calculated as the metabolic tumor volume (MTV). The average SUV in the lesion was defined as the SUVmean, and TLG was calculated as the product of SUVmean and MTV [6]. After calculating the TLG of all affected lesions, we summed the TLG of each lesion to generate a final TLG score for each patient.

Furthermore, as FDG is excreted into the urine, kidneys or urinary ducts show a physiologically high uptake of FDG; therefore, we considered that the physiological uptake of FDG in urine was inevitably included when evaluating kidney lesions. To account for this, two observers carefully excluded the urinary tract or a healthy area of kidney by the visual assessment based on a CT scan. Moreover, to minimize the influence of physiological urine uptake, we subtracted the FDG uptake of urine from that of each lesion. SUVmax of the lesions other than those of the kidney did not exceed 10.0 in the present study; therefore, we defined the areas with SUV > 10 as urine uptake. Finally, we calculated the TLG of

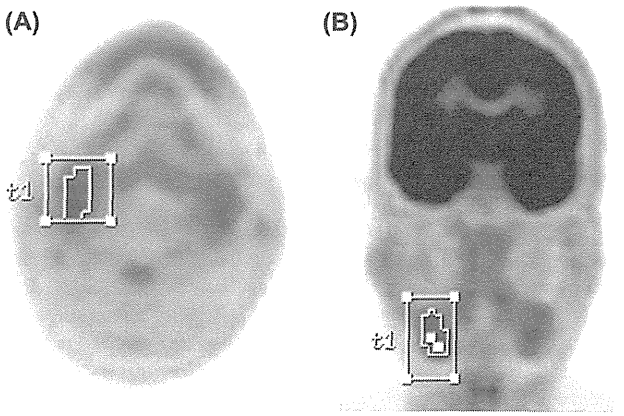

Figure 1. TLG measurement in a 47-year-old male with a salivary gland lesion. Sample coronal (A) and axial (B) PET images with quantitative parameters from a workstation are shown. Within the three-dimensional cuboid contour surrounding the right submandibular gland, voxels equal to or greater than the cut-off value (2.5) were automatically extracted. In this lesion, the maximum SUVmax, MTV, and TLG were 3.2, 6.5, and 18.1, respectively.

the area with an SUV > 10.0 within the contour and subtracted this from the TLG of the area with an SUV > 2.5. In addition, to completely exclude the influence of physiological urine excretion, we also performed sub-analysis in patients without renal lesions.

In this study, a maximum value of SUV within the region (SUVmax) of all affected organs was also assessed. When SUVmax was below 2.5, it was recorded as < 2.5. Owing to the methodological limitation, physiological excretion in the urine may influence SUVmax more strongly than TLG. Therefore, patients with kidney lesions were excluded when SUVmax was used in this analysis.

Laboratory data

Laboratory data were obtained from the medical records. The serum C-reactive protein (CRP), lactate dehydrogenase (LDH), soluble IL-2 receptor (sIL-2R), and IgG4 concentrations were included if the evaluations had been conducted within 2 months before FDG-PET/CT. Laboratory evaluations after FDG-PET/CT were allowed for those who did not receive treatment. Next, correlations between initial TLG or SUVmax values and serum markers were investigated in all patients.

All serum CRP and LDH tests were performed within 1 month before or after FDG-PET/CT. For sIL-2R and IgG4, 13 and 11 tests were performed within 1 month before or after FDG-PET/CT, respectively. Three and two cases lacked sIL-2R and IgG4 data, respectively.

Follow-up study

Among patients who underwent a follow-up FDG-PET/CT study, serial changes in TLG between initial and follow-up studies were evaluated and increasing or decreasing trends were assessed. Next, an assessment of each patient's course of global disease activity course was made from the 2 physicians' consensus. The course of disease activity was assessed based on image findings other than FDG-PET/CT, patients' symptoms, and physical finding [11]. The temporal change regarding each parameter was classified according to a three-grade system (improved, no change, or worsened), and the global disease course was determined by considering each temporal change. In brief, when classification of each parameter matched, the global disease course was judged according to that specific classification. When a conflicting case existed (such as a case when some parameters both improved and worsened), it was agreed that a decision would be made according to the most significant finding judged by each observer; however, no such case occurred within this study. We investigated whether the trend in serial TLG change and SUVmax change coincided with the global activity course.

Statistical analysis

Statistical analyses were performed using modified R software programs (The R Foundation for Statistical Computing, Perugia, Italy) as described previously [12,13]. Continuous data were presented as medians with interquartile ranges (IQR). The Spearman rank correlation coefficient test was used to analyze correlations between TLG and serum markers. A P-value of < 0.05 was considered statistically significant.

Results

Organs with abnormal FDG uptake

Organs with abnormal FDG uptake are listed in Table 2. Most affected organs exhibited positive FDG uptake, while there was no area with an SUV > 2.5 in any normal organ except for the kidney and intraorbital space (likely due to the physiological uptake of urine or external ocular muscles, respectively). Among these organs, the hilar and mediastinal lymph nodes were the most commonly affected, followed by the salivary glands. In contrast, three suspected lesions did not show abnormal FDG uptake. Two of these were typical of IgG4-RD lung involvement (one was a ground-glass opacity with interlobular septum thickening and reticular shadow and the other was a peribronchovascular infiltrative shadow with ill-defined nodules), and the third was a space-occupying pancreatic lesion with a 5-mm diameter that was identified by abdominal echography. Pathological examinations were not conducted for these three lesions.

Table 2. Organs with abnormal FDG uptake.

Organs with abnormal FDG uptake	n*
Lacrimal gland	1
Intraorbital space	3
Salivary gland	9
Pharyngolarynx	1
Supraclavicular lymph nodes	3
Hilar/mediastinal lymph nodes	13
Lung	2
Pancreas	1
Kidney	3
Thoracic aorta	1
Abdominal aorta	1
Retroperitoneal fibrosis	5
Prostate	5

*We counted multiple lesions within in a single organ as an one-organ lesion.

Quantitative analysis of FDG-PET/CT and serum markers

Quantitative analyses of the FDG-PET/CT and serum biomarker data are summarized in Table 3. The median MTV was 51.4 mL (20.2–92.5 mL) and TLG was 154.8 (63.7–324.4). The serum CRP (median: 0.2 mg/dL, IQR: 0.1–0.5 mg/dL) and LDH (median: 170 IU/L, IQR: 157–192 IU/L) levels were normal or slightly elevated in a majority of the cases. In contrast, elevated sIL2-R (median: 871.5 U/mL, IQR: 652.5 − 1337.5 U/mL) and IgG4 (median: 736 mg/dL, IQR: 539–1150 mg/dL) levels were observed.

Correlations between TLG and serum markers

Among the serum markers investigated in the present study, sIL-2R levels were found to significantly, positively correlate with TLG ($P = 0.001$, rs = 0.763) and SUVmax ($P = 0.018$, rs = 0.723). CRP ($P = 0.913$, rs = 0.029), LDH ($P = 0.444$, rs = − 0.199), and IgG4 ($P = 0.192$, rs = 0.357) levels did not significantly correlate with either TLG or SUVmax (Figure 2, Supplementary Figure 1 to be found online at http://informahealthcare.com/doi/abs/10.3109/14397595.2014.990674). Even when the two cases with the highest TLG were excluded from the analysis, the correlation between sIL-2R and TLG was still significant ($P = 0.030$, rs = 0.623).

Table 3. Summary of quantitative data.

Parameters	
MTV (ml)	51.4 (20.2–92.5)
TLG	154.8 (63.7–324.4)
Biomarkers	
CRP (mg/dl)	0.2 (0.1–0.5)
LDH (IU/l)	170 (157–192)
sIL-2R (U/ml)	871.5 (652.5–1337.5)
IgG4 (mg/dl)	736 (539–1150)

Values are presented as medians (interquartile ranges).
MTV metabolic tumor volume, *TLG* total lesion glycolysis, *sIL-2R* soluble interleukin-2 receptor, *IgG4* immunoglobulin G4.

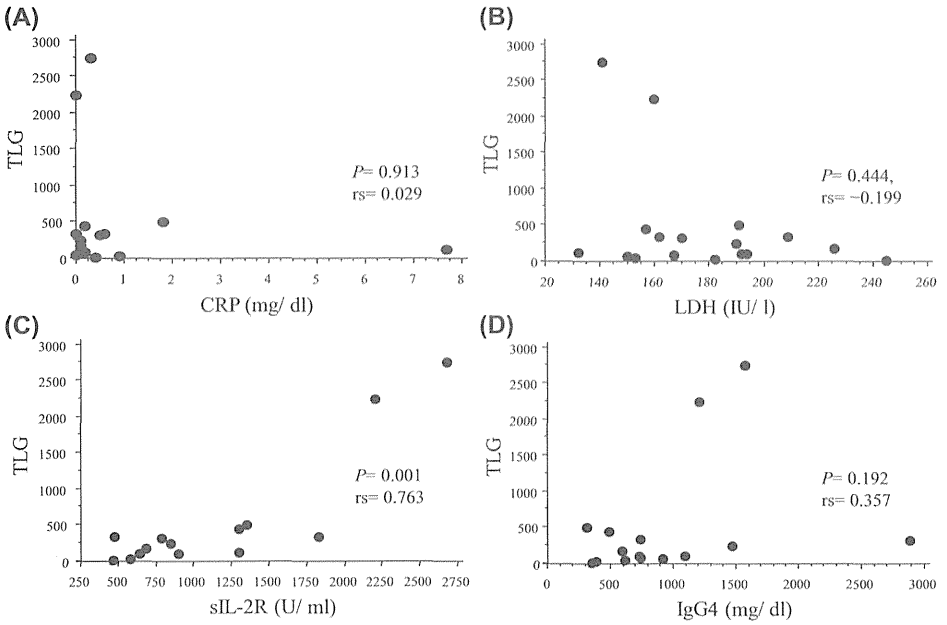

Figure 2. Correlations between TLG and serum biomarker levels. A: CRP, B: LDH, C: sIL-2R, D: IgG4. The serum sIL-2R level correlated significantly with TLG ($P = 0.001$, rs = 0.763), whereas no significant correlations were observed with the other markers. Each graph includes the rs and P values as determined using the Spearman rank correlation coefficient test.

We also performed the same analysis in patients without kidney lesions ($n = 15$). In this analysis, sIL-2R levels also correlated significantly with TLG ($P = 0.020$, rs = 0.717), whereas those of the other markers did not (Supplementary Figure 2 to be found online at http://informahealthcare.com/doi/abs/10.3109/14397595.2014.990674).

Serial changes in TLG or SUVmax coincident with the clinical course

Follow-up studies were performed in six patients in whom serial changes in TLG FDG-PET/CT were assessed (Table 4 and Supplementary Table 1 to be found online at http://informahealthcare.com/doi/abs/10.3109/14397595.2014.990674). Among these, three cases had received corticosteroid therapy and the others were followed up without therapy. Although intervals between the initial and follow-up studies were not uniform, reductions in TLG were observed in all cases that had received steroid therapy. In contrast, two of the three patients who did not receive steroid therapy showed increases in TLG. When comparing the trends in serial TLG changes with the global disease activity courses, all cases with decreased TLG were considered to have achieved improved global disease activity, whereas all cases with increased TLG were considered to have worsened. On the other hand, in two out of the five patients assessed, the course of SUVmax was not associated with the clinical course.

Discussion

In this study, we demonstrated that serum sIL-2R levels correlated significantly and positively with TLG. However, no other serum marker levels, including IgG4, correlated significantly with TLG. Serial changes in TLG paralleled clinical disease improvement or worsening. These results indicated the utility of TLG as a marker with which to monitor IgG4-RD activity. To the best of our knowledge, this was the first report to investigate the significance of TLG in IgG4-RD.

In IgG4-RD, although the symptoms are usually mild [14] and resolution is sometimes obtained naturally, as seen in the present study, adequately timed and intense treatment is needed to prevent the irreversible progression of fibrosis [15]. Therefore, evaluations of disease activity are important. However, IgG4-RD affects various organs; therefore, it is difficult to establish an integrated measurement that can evaluate severities of lesions in different organs. To date, several scoring systems have been pro-

Table 4. Serial change of TLG in clinical course.

	Treatment (+)			Treatment (−)		
	Case 1	Case 2	Case 3	Case 4	Case 5	Case 6
Age	66	73	77	73	54	53
Gender	Male	Male	Female	Male	Male	Female
Affected Organs	Kidney Pancreas	RF SG HMLN	OC Lung HMLN	OC	RF HMLN	Lung Pancreas
Test interval (month)	27	1	12	22	18	22
Initial dose of corticosteroid*	40	35	30	None	None	None
Initial TLG	86.5	154.8	324.4	11.9	108.7	0.0
Initial SUVmax	NA	5.9	8.9	4.6	10.0	<2.5
Follow-up TLG	66.9	8.0	157.6	10.6	591.5	16.8
Follow-up SUVmax	NA	3.0	5.2	4.9	5.0	3.2
Course of global activity	Improved	Improved	Improved	Improved	Worsened	Worsened

TLG total lesion glycolysis, *RF* retroperitoneal fibrosis, *SG* salivary glands, *HMLN* hilar and mediastinal lymph nodes, *OC* ocular cavity

Treatment (+) or (−) indicates whether corticosteroid therapy was initiated or not.

*Recorded when corticosteroid therapy was initiated during the period between initial and follow-up FDG-PET/CT. The corticosteroid dose was adjusted for prednisolone.

posed as tools for evaluating the global disease activity [11,16], but these systems have not been sufficiently established. Moreover, serum IgG4 level was included in the scoring, but in the present study, most of the cases did not undergo follow-up serum IgG4 measurements; therefore, the scoring systems were considered inapplicable. Accordingly, a physician's global assessment was used as a tool for evaluating changes in the disease activity [11,17].

FDG uptake is increased at sites of inflammation [18]. Elevated FDG uptake usually reflects more abundant glucose consumption, thereby indicating accelerated proliferation and increased metabolism [18–20]. Therefore, the degree of FDG uptake is considered to provide information about disease activity [21]. Actually, in some inflammatory diseases such as rheumatoid arthritis or Takayasu aortitis, FDG-PET was reported to have a diagnostic value and function effectively in evaluating treatment response [22–24].

Ebbo et al. performed a qualitative analysis of the FDG-PET/CT scans of IgG4-RD patients. The authors showed increased FDG uptake at the sites of affected lesions and reduced uptake after clinical remission was achieved [4]. Based on these results, they concluded that the FDG-PET/CT findings correlated with the disease activity. However, to date there have been no reports about the quantitative evaluation of FDG-PET/CT for IgG4-RD; therefore, we investigated the clinical significance of TLG in IgG4-RD.

SUVmax is a common and widely used quantitative analysis parameter of PET. This parameter is easily obtained, reproducible, and reader-independent, but it can be influenced by statistical noise. In addition, IgG4-RD patients are likely to have multiple organ involvement and thus multiple lesions. Because TLG is calculated as a summation of SUV of involved areas, we adopted and analyzed TLG as a quantitative value in this investigation.

Regarding the serum biomarkers, we demonstrated in the present study that serum sIL-2R levels strongly correlated with TLG. Although the precise biological role of sIL-2R remains unclear, the serum level of this receptor is considered as an indicator of lymphocyte activation [25] and elevated sIL-2R levels have been reported in several inflammatory diseases such as sarcoidosis [26] and systemic lupus erythematosus [25]. Moreover, elevated serum sIL-2R levels can predict sarcoidosis relapse after therapy [27]. Furthermore, in IgG4-RD, IL-2 is considered to have an important role in lymphocyte activation [28]. Matsubayashi et al. reported elevated serum sIL-2R levels in autoimmune pancreatitis patients and significant reductions in the level of this marker after corticosteroid therapy [29]. Autoimmune pancreatitis is now considered as a pancreatic manifestation of IgG4-RD [1]; therefore, sIL-2R might act as a biomarker of disease activity in IgG4-RD patients. The correlation between TLG and sIL-2R might thus indicate the utility of TLG as a biomarker in IgG4-RD.

In the previous studies, IgG4 is the most intensively investigated biomarker, and its serial changes in its levels were regarded as indicative of treatment responses or reactivation [30]. However, in the present study, IgG4 did not correlate significantly with TLG. The pathophysiological role of IgG4 remains unclear; however, IgG4 secretion is currently believed to occur in response to IL-10 stimulation, which acts to suppress immune responses [31]. Therefore, IgG4 may not directly reflect the intensity of inflammation. This indirect relationship might result in lack of correlation with TLG, although this idea is speculative.

In the analysis of serial FDG-PET/CT studies, all patients who exhibited decreases in TLG showed clinical improvement. On the contrary, two cases with increased TLG exhibited clinical deterioration. This result agreed with the above-described qualitative study [4], and suggested the utility of TLG as a parameter with which to monitor disease activity. On the other hand, in two cases the course of SUVmax was not associated with clinical course (Table 4). In these cases (Case 4 and 5), ocular movement and urinary tract obstruction improved or worsened in parallel with the change in TLG. We assume that the lesion volume might directly affect the function of these organs. In addition, after the treatment, case 2 showed a marked reduction in volume of the affected areas in parallel with TLG (from 154.8 to 8.0), whereas SUVmax showed just a moderate decrease (from 5.9 to 3.0); thus, TLG might exhibit a better association with global activity than SUVmax.

A major disadvantage of FDG-PET/CT is its high cost. Therefore, frequent and regular use of FDG-PET/CT is not possible in daily practice. Given the utility of sIL-2R and IgG4 in disease monitoring, measurement of these biomarkers may be advantageous in terms of cost and convenience compared with FDG-PET/CT. However, levels of both of these biomarkers might be elevated non-specifically because of other diseases or conditions [32,33]. Moreover, it is impossible to obtain site-specific information of activity when multiple lesions exist. In contrast, FDG-PET/CT can evaluate each organ separately [4]; therefore, it is comparatively easier to selectively investigate IgG4-RD lesion activities. For these reasons, serum biomarker evaluation is beneficial in daily practice, whereas more detailed FDG-PET/CT and TLG evaluation is useful as needed. On the other hand, it is still unclear whether comparing a TLG score in different organs has any clinical significance, because even lesions with a low TLG score could significantly aggravate patients (for example, intraorbital space lesions). Given this, further research is needed to better understand this problem.

This study has several limitations. First, this is a retrospective study with existing data deficits including the follow-up data of serum markers. Second, a pathological evaluation was not performed for all estimated lesions; therefore, sites of non-specific inflammation might have been included as IgG4-RD lesions. Third, the number of patients who participated in follow-up FDG-PET/CT studies was small, and intervals between the initial and follow-up FDG-PET/CT studies were not uniform; therefore, it was difficult to perform a statistical analysis regarding changes in TLG. Moreover, given the lack of information about the minimally clinically important difference in TLG, it was difficult to interpret the significance of a small change in TLG as seen in case 4. Fourth, SUV might be influenced by several factors such as the serum glucose level or the interval between the FDG injection and PET emission scan; therefore, the TLG calculations in the present study might exhibit a certain degree of fluctuation. In addition, physiological FDG uptake (such as urine) inevitably influenced TLG values, whereas SUV may show a low level even in the presence of definite lesions (such as interstitial pneumonia) and such lesions were omitted from analysis when SUV was below 2.5. Therefore, in cases where these lesions were present, an accurate evaluation was challenging. Despite these limitations, the present study showed a correlation between TLG and the sIL-2R level, and the serial change of TLG was associated with the clinical course. These findings indicated the utility of TLG for disease monitoring in IgG4-RD. In future studies, validations of these markers using clinically significant outcomes or parameters will be required.

Acknowledgments

We thank Drs. Y. Imura, M. Hashimoto, R. Nakashima, N. Yukawa, T. Nojima, D. Kawabata, T. Usui, K. Ohmura, and T. Fujii (Department of Rheumatology and Clinical Immunology, Graduate School of Medicine, Kyoto University) for their contributions to clinical practice.

Conflict of interest

The authors declare no conflict of interests. This study was supported by grants from the respiratory failure research group and the IgG4-related disease research group of the Ministry of Health, Labour and Welfare, Japan. The funding source did not have any role in the study design; in the collection, analysis, and interpretation of data; in the writing of the report; and in the decision to submit the article for publication.

References

1. Umehara H, Okazaki K, Masaki Y, Kawano M, Yamamoto M, Saeki T, et al. Comprehensive diagnostic criteria for IgG4-related disease (IgG4-RD), 2011. Mod Rheumatol. 2012;22(1):21–30.
2. Deshpande V, Zen Y, Chan JK, Yi EE, Sato Y, Yoshino T, et al. Consensus statement on the pathology of IgG4-related disease. Mod Pathol. 2012;25(9):1181–92.
3. Uchida K, Masamune A, Shimosegawa T, Okazaki K. Prevalence of IgG4-related disease in japan based on nationwide survey in 2009. Int J Rheumatol. 2012;2012:1–5.
4. Ebbo M, Grados A, Guedj E, Gobert D, Colavolpe C, Zaidan M, et al. Usefulness of 2-[18F]-fluoro-2-deoxy-D-glucose-positron emission tomography/computed tomography for staging and evaluation of treatment response in IgG4-related disease: a retrospective multicenter study. Arthritis Care Res (Hoboken). 2014;66(1):86–96.
5. Nakatani K, Nakamoto Y, Togashi K. Utility of FDG PET/CT in IgG4-related systemic disease. Clin Radiol. 2012;67(4):297–305.
6. Larson SM, Erdi Y, Akhurst T, Mazumdar M, Macapinlac HA, Finn RD, et al. Tumor treatment response based on visual and quantitative changes in global tumor glycolysis using PET-FDG imaging. The visual response score and the change in total lesion glycolysis. Clin. Positron Imaging. 1999;2(3):159–71.
7. Lee P, Weerasuriya DK, Lavori PW, Quon A, Hara W, Maxim PG, et al. Metabolic tumor burden predicts for disease progression and death in lung cancer. Int J Radiat Oncol Biol Phys. 2007;69(2):328–33.
8. Chung MK, Jeong HS, Park SG, Jang JY, Son YI, Choi JY, et al. Metabolic tumor volume of [18F]-Fluorodeoxyglucose positron emission tomography/computed tomography predicts short-term outcome to radiotherapy with or without chemotherapy in pharyngeal cancer. Clin Cancer Res. 2009;15:5861–8.
9. Seol YM, Kwon BR, Song MK, Choi YJ, Shin HJ, Chung JS, et al. Measurement of tumor volume by PET to evaluate prognosis in patients with head and neck cancer treated by chemo-radiation therapy. Acta Oncol. 2010;49(2):201–8.
10. Ryu IS, Kim JS, Roh J-L, Cho K-J, Choi S-H, Nam SY, et al. Prognostic significance of preoperative metabolic tumour volume and total lesion glycolysis measured by 18F-FDG PET/CT in squamous cell carcinoma of the oral cavity. Eur J Nucl Med Mol Imaging. 2013;41(3):4521–61.
11. Khosroshahi A, Carruthers MN, Deshpande V, Unizony S, Bloch DB, Stone JH. Rituximab for the treatment of IgG4-related disease. Medicine. 2012;91(1):57–66.
12. Scrucca L, Santucci A, Aversa F. Competing risk analysis using R: an easy guide for clinicians. Bone Marrow Transplant. 2007;40:381–7.
13. EZR_HP. http://www.jichi.ac.jp/saitama-sct/SaitamaHP.files/statmed.html; 2013 Oct pp. 1–1. Report No.: Accessed on 2013 Oct 1.
14. Umehara H, Okazaki K, Masaki Y, Kawano M, Yamamoto M, Saeki T, et al. A novel clinical entity, IgG4-related disease (IgG4RD): general concept and details. Mod Rheumatol. 2012;22(1):1–14.
15. Shimizu Y, Yamamoto M, Naishiro Y, Sudoh G, Ishigami K, Yajima H, et al. Necessity of early intervention for IgG4-related disease–delayed treatment induces fibrosis progression. Rheumatology. 2013;52(4):679–83.
16. Carruthers MN, Stone JH, Deshpande V, Khosroshahi A. Development of an IgG4-RD Responder Index. Int J Rheumatol. 2012;2012:259408.
17. Ebbo M, Daniel L, Pavic M, Sève P, Hamidou M, Andres E, et al. IgG4-related systemic disease: features and treatment response in a French cohort: results of a multicenter registry. Medicine. 2012;91(1):49–56.
18. Signore A, Glaudemans AWJM. The molecular imaging approach to image infections and inflammation by nuclear medicine techniques. Ann Nucl Med. 2011;25(10):681–700.
19. Yamada S, Kubota K, Kubota R, Ido T, Tamahashi N. High accumulation of fluorine-18-fluorodeoxyglucose in turpentine-induced inflammatory tissue. J Nucl Med. 1995;36(7):1301–6.
20. Ishimori T, Saga T, Mamede M, Kobayashi H, Higashi T, Nakamoto Y, et al. Increased 18F-FDG uptake in a model of inflammation: concanavalin A-mediated lymphocyte activation. J Nucl Med. 2002;43:658–63.
21. Weber WA, Schwaiger M, Avril N. Quantitative assessment of tumor metabolism using FDG-PET imaging. Nucl Med Biol. 2000;27(7):683–7.
22. Cheng Y, Lv N, Wang Z, Chen B, Dang A. 18-FDG-PET in assessing disease activity in Takayasu arteritis: a meta-analysis. Clin Exp Rheumatol. 2013;31(1 Suppl 75):S22–7.
23. Wang S-C, Xie Q, Lv W-F. Positron emission tomography/computed tomography imaging and rheumatoid arthritis. Int J Rheum Dis. 2014;17(3):248–55.
24. Santhosh S, Mittal BR, Gayana S, Bhattacharya A, Sharma A, Jain S. F-18 FDG PET/CT in the evaluation of Takayasu arteritis: An experience from the tropics. J Nucl Cardiol. 2014;21(5):993–1000.
25. Smith MF, Hiepe F, Dörner T, Burmester G. Biomarkers as tools for improved diagnostic and therapeutic monitoring in systemic lupus erythematosis. Arthritis Res Ther. 2009;11(6):255.
26. Junghans RP, Waldmann TA. Metabolism of Tac (IL2Ralpha): physiology of cell surface shedding and renal catabolism, and suppression of catabolism by antibody binding. J Exp Med. 1996;183(4):1587–602.
27. Vorselaars ADM, Verwoerd A, Van Moorsel CHM, Keijsers RGM, Rijkers GT, Grutters JC. Prediction of relapse after discontinuation of infliximab therapy in severe sarcoidosis. Eur Respir J. 2014;43:602–9.
28. Okazaki K, Uchida K, Koyabu M, Miyoshi H, Takaoka M. Recent advances in the concept and diagnosis of autoimmune pancreatitis and IgG4-related disease. J Gastroenterol. 2011;46:277–88.
29. Matsubayashi H, Uesaka K, Kanemoto H, Asakura K, Kakushima N, Tanaka M, et al. Soluble IL-2 receptor, a new marker for autoimmune pancreatitis. Pancreas. 2012;41(3):493–6.
30. Tabata T, Kamisawa T, Takuma K, Egawa N, Setoguchi K, Tsuruta K, et al. Serial changes of elevated serum IgG4 levels in IgG4-related systemic disease. Intern Med. 2011;50(2):69–75.
31. Zen Y, Nakanuma Y. IgG4-related disease: a cross-sectional study of 114 cases. Am. J Surg Pathol. 2010;34(12):1812–9.
32. Yamamoto M, Tabeya T, Naishiro Y, Yajima H, Ishigami K, Shimizu Y, et al. Value of serum IgG4 in the diagnosis of IgG4-related disease and in differentiation from rheumatic diseases and other diseases. Mod Rheumatol. 2011;22(3):419–25.
33. Ryuko H, Otsuka F. A comprehensive analysis of 174 febrile patients admitted to Okayama University Hospital. Acta Med Okayama. 2013;67(4):227–37.

Supplementary material available online

Supplementary Figures 1, 2 and Table 1.

Journal of Human Genetics (2014) 59, 107–109

www.nature.com/jhg

SHORT COMMUNICATION

Significant association between *CYP3A5* polymorphism and blood concentration of tacrolimus in patients with connective tissue diseases

Kosuke Tanaka[1], Chikashi Terao[1], Koichiro Ohmura[2], Meiko Takahashi[1], Ran Nakashima[2], Yoshitaka Imura[2], Hajime Yoshifuji[2], Naoichiro Yukawa[2], Takashi Usui[2], Takao Fujii[2], Tsuneyo Mimori[2] and Fumihiko Matsuda[1]

Although the association between *CYP3A5* polymorphism and blood concentration of tacrolimus (TAC) in patients with solid organ transplantation was established, whether the association is also true in patients with connective tissue disease (CTD) who usually receive small amount of TAC is uncertain. Here, we performed a quantitative linear regression analysis to address the association between *CYP3A5* and blood TAC concentration in patients with CTD. A total of 72 patients with CTD were recruited in the current study and genotyped for rs776746 in *CYP3A5*, which showed strong association with TAC concentration in patients with solid organ transplantation. The blood trough concentration of TAC after taking 3 mg per day was retrospectively obtained for each patient. As a result, allele A of rs776746 showed a significant association with a decreasing blood concentration of TAC ($P=0.0038$). Those who are carrying at least one copy of the A allele displayed decreased mean concentration of TAC by 31.0% compared with subjects with GG genotype. Rs776746 is associated with concentrations of TAC in patients with CTD.
Journal of Human Genetics (2014) **59**, 107–109; doi:10.1038/jhg.2013.129; published online 19 December 2013

Keywords: connective tissue disease; pharmacogenetics; tacrolimus

Tacrolimus (FK506, TAC) is a calcineurin inhibitor isolated from *Streptomyces tsukubaensis*[1] and one of the many types of powerful immunosuppressants that are frequently used for solid organ transplantation to prevent organ rejection.[2] TAC is also used for patients with connective tissue disease (CTD) including rheumatoid arthritis (RA), systemic lupus erythematosus, polymyositis and dermatomyositis to control disease activity.[3,4] TAC is metabolized mainly by cytochrome P450 (CYP) 3A in the liver and intestine.[5] Because TAC concentration is highly variable among patients, to predict TAC concentration to achieve therapeutic effect is a big challenge. Previous studies revealed that the variation of TAC concentration is largely attributable to different expressions of *CYP3A* in patients of organ transplantation. Patients carrying *CYP3A5*3* determined by the G allele of rs776746 were shown to have high TAC concentration than patients with the A allele.[5,6] Although TAC is a substrate for P-glycoprotein encoded by the *ABCB1* gene, effects of polymorphisms in *ABCB1* on TAC concentration are inconclusive.[6–8] Genetic studies have been performed mainly recruiting patients with organ transplantation to date. The number of previous studies focusing on TAC concentration in non-organ transplantation subjects is limited.[9,10]

When TAC is given to patients with CTD, the dosage is around 3 mg per day,[3,4] which is much lower than that given to patients of organ transplantation. For example, patients with renal transplantation receive 0.3 mg kg^{-1} per day at the transplantation and 0.12 mg kg^{-1} per day as maintainance.[11] In addition, although recipients of renal transplantation take TAC twice daily,[11] patients with only CTD take a single dose of TAC per day. The effect of *CYP3A5* on TAC concentrations with low TAC exposure in patients with CTD has not been studied so far. Furthermore, chronic, systemic and autoimmune inflammatory process in CTD may influence the metabolism and concentration of TAC. Thus, whether the association between polymorphisms of *CYP3A5* and TAC concentrations can be observed in patients with CTD remained unclear. Here, we performed an association study to address this point.

This study was designed in accordance with the Helsinki Declaration and approved by the ethics committee of Kyoto University Graduate School and Faculty of Medicine. A total of 72 subjects with CTD who were prescribed to take a single dose of 3 mg of TAC every day in the evening at the Department of Rheumatology and Clinical Immunology, Kyoto University Graduate School of Medicine from December 2005 to December 2012 were enrolled in this study. Written informed consent was obtained from all the participants. Patients

[1]Center for Genomic Medicine, Kyoto University Graduate School of Medicine, Kyoto, Japan and [2]Department of Rheumatology and Clinical Immunology, Kyoto University Graduate School of Medicine, Kyoto, Japan
Correspondence: Dr C Terao, Center for Genomic Medicine, Kyoto University Graduate School of Medicine, Kyoto 606-8507, Japan.
E-mail: a0001101@kuhp.kyoto-u.ac.jp
Received 26 September 2013; revised 25 November 2013; accepted 25 November 2013; published online 19 December 2013

took PROGRAF (Astellas Pharma Inc., Tokyo, Japan) capsules containing 1 or 0.5 mg TAC. CTD patients fulfilled criteria for each disease, namely, American College of Rheumatology (ACR) criteria for RA in 1987[12] or ACR/EULAR criteria in 2010,[13] for systemic lupus erythematosus,[14] polymyositis and dermatomyositis[15] and for polyarteritis nodosa and microscopic polyangiitis.[16] Information of age, sex, weight, serum creatinine and date of prescription, dosage, and blood concentration of TAC were obtained from clinical charts retrospectively by the system previously described.[17] Information of prescription and dosage of corticosteroid was also obtained. TAC concentration data were obtained at least one week after prescription was initiated or changed. The data of concurrent use of cyclosporine or bosentan, contraindication due to interaction with TAC, was excluded. Estimated glomelular filtration ratio (eGFR) was inferred by serum creatinine, age and sex. The blood trough TAC concentration with 3 mg TAC (around 12 h after taking TAC) was used. TAC concentrations were quantified by two measurements according to measuring time; namely, microparticle enzyme immunoassay (MEIA, IMxTM-TACRO II, Abbott Laboratories, Green Oaks, IL, USA) until May 2009 and chemiluminescent immunoassay (CLIA, ARCHITECT_TACRO, Abbott Laboratories) from May 2009. These measurements can quantify even low TAC concentrations ($\sim$1.5 and $\sim$0.5 ng ml^{-1}, respectively). When TAC concentrations were available for both measurements in a patient, data of CLIA with lower measuring limit of TAC concentrations was used. A total of 63 and 9 patients were quantified by CLIA and MEIA, respectively (hereafter termed as CLIA group and MEIA group, respectively). When multiple TAC concentrations were available, the mean of them was adopted. Calculations were performed on the basis of logarithm of TAC concentrations to obtain normal distribution and to avoid excess influence of extreme data.

The summary of the subjects in the current study is shown in Table 1. Log-transformation of TAC concentration supported applying linear regression analysis. When we analyzed correlations between TAC concentration and age, sex, weight, eGFR, dosage or usage of corticosteroid or the presence of RA or systemic lupus erythematosus by single linear regression analysis, none of them displayed overall significant associations ($P \geqslant 0.083$). However, because presence of RA showed a suggestive association in MEIA group ($P = 0.0091$), we used presence of RA as a covariate. Rs776746, whose G allele determined *CYP3A5*3*, was selected on the basis of previous studies and genotyped by the Taqman assay (Applied Biosystems Inc, Foster city, CA, USA). As a result, no deviation from Hardy–Weinberg equilibrium was observed ($P = 0.13$). Although previous reports comparing different measurement methods of blood concentration of TAC showed good correlations ($r \geqslant 0.84$) and did not detect discrepancy even in ranges of low concentrations,[18,19] MEIA was suggested to underestimate TAC concentrations in low levels.[19] Thus we analyzed the associations in CLIA and MEIA groups separately, and the overall associations were estimated by meta-analysis using inverse-variance method. We found a significant decreasing effect of the A allele of rs776746 on TAC concentration ($P = 0.0038$, Figure 1). Both MEIA and CLIA groups showed the comparable effect sizes, supporting the accuracy of the result (Table 2). Patients who carried A allele had 31.0% lower mean concentration than those who were homozygote for G allele. Although the current and the previous studies[11] showed a good fit of the dose-dependent model of rs776746, there are also conflicting reports.[6,20] Considering the limited number of subjects with AA genotype, the dose-dependent effect of rs776746 should be regarded as inconclusive. Meta-analysis of the recessive model resulted in a comparable result ($P = 0.0035$, AA + GA vs GG).

The current study provided evidence that TAC concentration was strongly influenced by *CYP3A5* in patients with CTD even taking a small amount of TAC. Our results showed the same direction of A allele of rs776746 and comparable effect sizes in the previous studies using patients of solid organ transplantation.[5,6] Disease-specific influence on TAC concentrations was not clear. As this study contained relatively small number of subjects and low TAC concentrations around the measurement limits might be associated with diminished accuracy, these results should be replicated by a larger number of patients with CTD, also including other populations. Because the predictive model of TAC concentration is proposed in

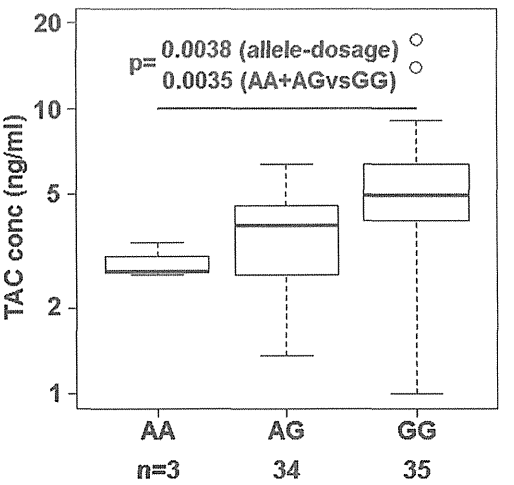

Figure 1 Association between TAC concentration and the polymorphism in *CYP3A5* in patients with CTD. The obtained or inferred TAC concentrations adjusted for 3mg TAC are shown according to rs776746 genotypes. *Y* axis is shown in log scale. The mean concentrations are 2.88, 3.57 and 5.10 ng ml^{-1} for AA, AG and GG genotypes, respectively. TAC concentrations were adjusted for MEIA group.

Table 1 Summary of subjects in the current study

	Study subjects
Age[a]	48.94 ± 17.24
Sex	Male 13, female 59
Disease	RA: 22, SLE: 43, DM: 3, PM: 2, PAN: 1, mPA: 1

Abbreviations: DM, dermatomyositis; mPA, microscopic polyangiitis; PAN, polyarteritis nodosa; PM, polymyositis; RA, rheumatoid arthritis; SLE, systemic lupus.erythematosus.
[a]mean ± s.d.

Table 2 Association between rs776746 and TAC concentration in multiple regression analysis

	Number	*Beta*	*s.e.*	P-*value*
CLIA	63	0.106	0.041	0.012
MEIA	9	0.161	0.12	0.22
Overall	72	0.112	0.039	0.0038

Abbreviations: CLIA, chemiluminescent immunoassay; MEIA, microparticle enzyme immunoassay; TAC, tacrolimus.
Statistics adjusted by rheumatoid arthritis presence.

patients of organ transplantation, it will be interesting to construct a predictive model of TAC concentration in patients with CTD.

CONFLICT OF INTEREST

The authors declare no conflict of interest.

ACKNOWLEDGEMENTS

We would like to thank all the patients registered in this study. This study was supported by Kyoto University Step-up grant.

1 Kino, T., Hatanaka, H., Miyata, S., Inamura, N., Nishiyama, M., Yajima, T. *et al.* FK-506, a novel immunosuppressant isolated from a Streptomyces. II. Immunosuppressive effect of FK-506 in vitro. *J. Antibiot. (Tokyo)* **40,** 1256–1265 (1987).
2 Scott, L. J., McKeage, K., Keam, S. J. & Plosker, G. L. Tacrolimus: a further update of its use in the management of organ transplantation. *Drugs* **63,** 1247–1297 (2003).
3 Takeuchi, T., Kawai, S., Yamamoto, K., Harigai, M., Ishida, K. & Miyasaka, N. Post-marketing surveillance of the safety and effectiveness of tacrolimus in 3,267 Japanese patients with rheumatoid arthritis. *Mod. Rheumatol.* **24,** 8–16 (2014).
4 Takahashi, S., Hiromura, K., Sakurai, N., Matsumoto, T., Ikeuchi, H., Maeshima, A. *et al.* Efficacy and safety of tacrolimus for induction therapy in patients with active lupus nephritis. *Mod. Rheumatol.* **21,** 282–289 (2011).
5 Hesselink, D. A., van Gelder, T. & van Schaik, R. H. The pharmacogenetics of calcineurin inhibitors: one step closer toward individualized immunosuppression? *Pharmacogenomics* **6,** 323–337 (2005).
6 Tsuchiya, N., Satoh, S., Tada, H., Li, Z., Ohyama, C., Sato, K. *et al.* Influence of CYP3A5 and MDR1 (ABCB1) polymorphisms on the pharmacokinetics of tacrolimus in renal transplant recipients. *Transplantation* **78,** 1182–1187 (2004).
7 Tada, H., Tsuchiya, N., Satoh, S., Kagaya, H., Li, Z., Sato, K. *et al.* Impact of CYP3A5 and MDR1(ABCB1) C3435T polymorphisms on the pharmacokinetics of tacrolimus in renal transplant recipients. *Transplant. Proc.* **37,** 1730–1732 (2005).
8 Vafadari, R., Bouamar, R., Hesselink, D. A., Kraaijeveld, R., van Schaik, R. H., Weimar, W. *et al.* Genetic polymorphisms in ABCB1 influence the pharmacodynamics of tacrolimus. *Ther. Drug. Monit.* **35,** 459–465 (2013).
9 Hirai, F., Takatsu, N., Yano, Y., Satou, Y., Takahashi, H., Ishikawa, S. *et al.* CYP3A5 genetic polymorphisms affect the pharmacokinetics and short-term remission in patients with ulcerative colitis treated with tacrolimus. *J. Gastroenterol. Hepatol.* (in press).
10 Shi, X. J., Geng, F., Jiao, Z., Cui, X. Y., Qiu, X. Y. & Zhong, M. K. Association of ABCB1, CYP3A4*18B and CYP3A5*3 genotypes with the pharmacokinetics of tacrolimus in healthy Chinese subjects: a population pharmacokinetic analysis. *J. Clin. Pharm. Ther.* **36,** 614–624 (2011).
11 Niioka, T., Kagaya, H., Miura, M., Numakura, K., Saito, M., Inoue, T. *et al.* Pharmaceutical and genetic determinants for interindividual differences of tacrolimus bioavailability in renal transplant recipients. *Eur. J. Clin. Pharmacol.* **69,** 1659–1665 (2013).
12 Arnett, F. C., Edworthy, S. M., Bloch, D. A., McShane, D. J., Fries, J. F., Cooper, N. S. *et al.* The American Rheumatism Association 1987 revised criteria for the classification of rheumatoid arthritis. *Arthritis. Rheum.* **31,** 315–324 (1988).
13 Aletaha, D., Neogi, T., Silman, A. J., Funovits, J., Felson, D. T., Bingham, C. O. 3rd *et al.* Rheumatoid arthritis classification criteria: an American College of Rheumatology/European League Against Rheumatism collaborative initiative. *Arthritis. Rheum.* **62,** 2569–2581 (2010).
14 Hochberg, M. C. Updating the American College of Rheumatology revised criteria for the classification of systemic lupus erythematosus. *Arthritis. Rheum.* **40,** 1725 (1997).
15 Bohan, A. & Peter, J. B. Polymyositis and dermatomyositis (first of two parts). *N. Engl. J. Med.* **292,** 344–347 (1975).
16 Bloch, D. A., Michel, B. A., Hunder, G. G., McShane, D. J., Arend, W. P., Calabrese, L. H. *et al.* The American College of Rheumatology 1990 criteria for the classification of vasculitis. Patients and methods. *Arthritis. Rheum.* **33,** 1068–1073 (1990).
17 Terao, C., Hashimoto, M., Yamamoto, K., Murakami, K., Ohmura, K., Nakashima, R. *et al.* Three groups in the 28 joints for rheumatoid arthritis synovitis–Analysis using more than 17,000 assessments in the KURAMA database. *PLoS One* **8,** e59341 (2013).
18 Ju, M. K., Chang, H. K., Kim, H. J., Huh, K. H., Ahn, H. J., Kim, M. S. *et al.* Is the affinity column-mediated immunoassay method suitable as an alternative to the microparticle enzyme immunoassay method as a blood tacrolimus assay? *Transplant. Proc.* **40,** 3673–3678 (2008).
19 Marubashi, S., Nagano, H., Kobayashi, S., Eguchi, H., Takeda, Y., Tanemura, M. *et al.* Evaluation of a new immunoassay for therapeutic drug monitoring of tacrolimus in adult liver transplant recipients. *J. Clin. Pharmacol.* **50,** 705–709 (2010).
20 Hesselink, D. A., van Schaik, R. H., van der Heiden, I. P., van der Werf, M., Gregoor, P. J., Lindemans, J. *et al.* Genetic polymorphisms of the CYP3A4, CYP3A5, and MDR-1 genes and pharmacokinetics of the calcineurin inhibitors cyclosporine and tacrolimus. *Clin. Pharmacol. Ther.* **74,** 245–254 (2003).

DISCLOSURE

All authors disclosed no financial relationships relevant to this publication.

Kenichiro Imai, MD
Masaki Tanaka, MD
Naomi Kakushima, MD, PhD
Kohei Takizawa, MD
Hiroyuki Matsubayashi, MD, PhD
Kinichi Hotta, MD
Yuichiro Yamaguchi, MD
Hiroyuki Ono, MD, PhD
Division of Endoscopy
Shizuoka Cancer Center
Nagaizumi, Suntogun
Shizuoka, Japan

REFERENCES

1. Imai K, Tanaka M, Hasuike N, et al. Feasibility of a "resect and watch" strategy with endoscopic resection for superficial pharyngeal cancer. Gastrointest Endosc 2013;78:22-9.
2. Edge SB, Compton CC, Fritz AG, et al., editors. AJCC Cancer Staging Manual, 7th ed. New York: Springer; 2010.
3. Muto M, Satake H, Yano T, et al. Long-term outcome of transoral organ-preserving pharyngeal endoscopic resection for superficial pharyngeal cancer. Gastrointest Endosc 2011;74:477-84.
4. Katada C, Tanabe S, Koizumi W, et al. Narrow band imaging for detecting superficial squamous cell carcinoma of the head and neck in patients with esophageal squamous cell carcinoma. Endoscopy 2010;42:185-90.

http://dx.doi.org/10.1016/j.gie.2013.09.001

Gastroesophageal acid reflux mainly occurs on the right side of the esophagus

To the Editor:

We read with great interest the study by Cassani et al[1] describing the asymmetric circumferential distribution of Barrett's neoplasms. The results of their study suggest the importance of endoscopic examination of the right side wall of the esophagus, not only in patients with short-segment Barrett's esophagus (SSBE) but also those with long-segment Barrett's esophagus (LSBE), for detecting early-stage adenocarcinomas.

Our group is also interested in the asymmetrical circumferential distribution of various esophagogastric lesions, and we first published a study in 2006 that investigated the prevalence of esophageal mucosal breaks in patients with different grades of reflux esophagitis.[2] In that investigation, we found that the mucosal breaks of low-grade esophagitis occurred mainly on the right anterior wall of the distal esophagus. Our observation was later confirmed in 2007 by Edebo et al.[3]

We also investigated the asymmetrical circumferential distribution of SSBE with tonguelike configurations and in 2008 reported that tonguelike SSBE were mainly found on the right anterior side wall of the esophagus.[4] In 2006, we examined the localization of early-stage neoplastic Barrett's lesions in patients with SSBE and reported their predominant distribution on the right anterior wall of the esophagus.[5] That finding was soon confirmed in 2007 by Pech et al.[6]

In addition to reflux esophagitis and Barrett's adenocarcinomas, we investigated the circumferential distribution of ruptured esophageal varices as possible acid-related lesions. The administration of proton pump inhibitors has been repeatedly reported to decrease the risk of esophageal variceal rupture, whereas esophageal acid reflux has been speculated to induce esophageal erosions and rupture of the varices. In our study population, high-grade esophageal varices with risk of rupture were most frequently found on the right posterior wall of the distal esophagus. However, it is quite interesting that ruptured esophageal varices were most frequently found on the right anterior wall of the esophagus.[7]

These findings, including the predominant right anterior localization of mucosal breaks of reflux esophagitis, tonguelike SSBE lesions, Barrett's neoplasia, and ruptured esophageal varices, suggest the presence of right anterior predominant gastroesophageal acid reflux in the distal esophagus. To investigate the radially asymmetrical distribution of gastroesophageal acid reflux, we developed a novel pH sensor catheter equipped with 8 pH sensors on its surface and have studied acid exposure time in different radial walls of the esophagus in patients with reflux esophagitis.[8,9] By using our device, we found that acid reflux was most prominent on the right anterior wall of the esophagus and nicely coincided with the locations of mucosal breaks in individual patients. The mechanism by which gastric acid reflux occurs mainly on the right anterior wall of the distal esophagus has not been completely clarified. Nevertheless, the asymmetrical compression pressure produced by the lower esophageal sphincter and diaphragmatic hiatus may play a role in the asymmetrical reflux of gastric contents.

In their study, Cassani et al[1] extended this concept from the distal esophagus to the more proximal esophagus and found that Barrett's neoplasia associated with LSBE was also predominantly present on the right anterior wall of the esophagus. An interesting point about their study, which is open for possible discussion, is the method used to divide the patients into 2 groups: neoplasia associated with SSBE and that with LSBE, based on the conventional point 3 centimeters above the lower esophageal sphincter. In the upper portion of the esophagus, more than 3 centimeters above the LES, refluxed gastric contents are expected to be more uniformly distributed in all circumferential directions of the esophagus. Therefore, in the upper esophagus, the asymmetrical distribution of